Water Research 190 (2021) 116727

Contents lists available at ScienceDirect

Water Research

journal homepage: www.elsevier.com/locate/watres

Nutrient delivery efficiency of a combined sewer along a lake challenged by incipient eutrophication

Marco Pilotti[a,*], Laura Barone[a], Matteo Balistrocchi[b], Giulia Valerio[a], Luca Milanesi[a], Daniele Nizzoli[c]

[a] DICATAM, Department of Civil, Environmental, Architectural Engineering and Mathematics, University of Brescia, via Branze 43, 25123 Brescia, Italy
[b] Department of Engineering Enzo Ferrari, University of Modena and Reggio Emilia, via Vivarelli 10, 41125 Modena, Italy
[c] Department of Chemistry, Life Sciences and Environmental Sustainability, University of Parma, Parco Area delle Scienze 11/A, 43124 Parma, Italy

ARTICLE INFO

Article history:
Received 13 July 2020
Revised 1 December 2020
Accepted 2 December 2020
Available online 3 December 2020

Keywords:
Combined sewers
Infiltration waters
Hydraulic simulation
Monitoring campaign
Nutrient load
Lake eutrophicatio

ABSTRACT

Although sewage diversion outside of a lake's watershed is now ordinary practice in the restoration of eutrophic lakes, often the observed recovery is slower than expected and the internal load from the lake anoxic sediments is identified as a possible reason. However, in the case of combined sewer, the quantification of the residual nutrient load discharged from sewer spillways must also be questioned. In this paper, the diversion efficiency of the sewer system along the east coast of Lake Iseo, a prealpine Italian lake where eutrophication effects are still severe, is investigated. To this purpose, a representative part of the sewer system was modelled by PCSWMM and calibrated by using an extensive series of discharge measurements. Water quality monitoring during wet weather periods reveals that the first flush is common in tributary sewers, whereas it is absent along the main collector. Moreover, flow discharges are strongly affected by infiltration waters, which are controlled by the lake water level. The calibrated model, including infiltration modeling, was used to assess the annual overflow volumes and the nutrient load through a continuous 10-year simulation. Simulations were conducted both with regard to the current conditions and to a climate change scenario. Results show that the discharged residual load is at least 7 times larger than the design value, with the water infiltration contributing to 17% to the overflow volume and that non-structural practices could considerably reduce the overall impact of the sewer. This research thus provides important insight into the potential impact of combined sewer overflows on lacustrine environments and addresses effective mitigation measures in similar contexts.

1. Introduction

Eutrophication has been recognized as the greatest challenge to the integrity of water resources since the late '60s of the last century (e.g., Welch, 1981; Schindler, 1977, 2006, 2012; McCrackin et al., 2017), affecting both inland freshwaters and coastal marine ecosystems. Owing to their long renewal time and suitability to human settlings and activities, lakes are particularly sensitive to this phenomenon. Worldwide, most lakes have shown an increase in their trophic level, often with a strong impairment of their ecological services (e.g., Jenny et al., 2020). According to the Joint International Lake Environment Committee / United Nations Environment Program project "Survey of the State of World Lakes", all 217 major lakes included in the survey demonstrated to be affected by eutrophication (e.g., Matsui et al., 1995). Due to their role in phytoplankton growth, phosphorus (P) and nitrogen (N) along with their stoichiometry, are considered to be the crucial nutrients that control the eutrophication development (e.g., Schindler, 2006, 2012), therefore, costly actions to reduce their loads have been extensively undertaken.

Urban sewage is widely acknowledged as a relevant nutrient source and a leading cause of generalized environmental degradation (Walsh et al., 2005). Even in the presence of agricultural non-point sources, due to the imperviousness of urban areas, the relative contribution of the urban pollution load to the total load largely exceeds the ratio between the urbanized catchment area and the total catchment area. For instance, Meals and Budd (1998) estimated for Lake Champlain that urban sewage contributes to 18% of the phosphorous load, while the urbanized catchment area is only about 3% of the total catchment extension.

* Corresponding author.
E-mail address: marco.pilotti@unibs.it (M. Pilotti).

https://doi.org/10.1016/j.watres.2020.116727

In historical settlements around European lakes, the urban drainage network is frequently made up of combined sewer systems (CSSs), draining relatively small tributary sub-catchments (Marsalek, 2003). Such CSSs are interconnected by a diversion pipe, herein referred to as a main collector, placed along the lake shoreline and featuring a large conveyance capacity. This pipe intercepts sewage from tributary sub-catchments, which otherwise would directly enter the lake, and delivers it to an end-of-pipe wastewater treatment plant (WWTP). Treated waters are finally discharged, when possible, outside of the lake watershed. However, during wet weather periods, the untreated mixture of storm waters and waste waters, exceeding either the CSS conveyance capacity or the WWTP processing capacity, is discharged into the lake waters as combined sewer overflows (CSOs) by means of spillways.

The presence of spillways, along the main diversion pipe and upstream of the tributary CSS connections, is justified by technical and economic reasons. Nevertheless, urban storm waters are well-known pollutant drivers (Novotny and Goodrich-Mahoney, 1978; Marsalek and Chocat, 2002; Tang et al., 2005; Kaushal et al., 2011), which wash the atmosphere, the impermeable surfaces, and the drainage pipes thus mobilizing sediments that settled during dry weather periods. Therefore, during wet weather periods, CSOs may deliver large amounts of pollutants in addition to those delivered by waste waters (e.g., Bryan Ellis and Yu, 1995; Chebbo et al., 2001; Kim et al., 2007) and their cumulative impact cannot be disregarded (Tibbetts, 2005; USEPA, 2009), especially when the receiving surface waters are characterized by long renewal times. When the final recipient is a lake, characterised by integrative mechanisms, the total discharged load is of major concern. Indeed, typical water renewal times for lakes lie in the order of years (with respect to days for rivers) and this is particularly true in deep lakes (e.g., Pilotti et al., 2014).

Further, when a CSS is partially or totally submerged by the water table, its hydraulic load can be affected by infiltration waters. Especially when the CSS is old, infiltration waters through cracked pipes, leaky joints and poor manhole connections, may overload the conduits and diminish the actual conveyance capacity, increasing the CSOs number and volume with respect to the design assumption. Kidmose et al. (2015) have shown that in the City of Silkeborg, Western Denmark, one fourth of water input to the storm water runoff systems comes from groundwater sources. This improper discharge (Karpf and Krebs, 2011; Xu et al., 2014) is particularly relevant in lacustrine environments, where pipes are usually located along the lake shoreline and the water table is controlled by the lake level.

Usually, the contribution of infiltration waters to the CSS discharge is disregarded in spillway design, and storm waters are supposed to dilute waste water pollutants. Owing to the systematic use of these assumptions, the environmental impact of CSOs on lakes has often been underestimated. Moreover, CSOs contribute to mosquito growth, increase the risk of insect-borne disease transmission (Lund et al., 2014), cause closures of areas suitable for swimming, as a result of elevated *Escherichia coli* levels (McLellan et al., 2007; Sebastiá-Frasquet et al., 2013), affect the amenity of wetlands and cause the reduction of dissolved oxygen (Camargo and Alonso, 2006; Smil, 2000; Paul and Meyer, 2001). Over the long term, they also lead to a dramatic change in aquatic community composition (Lund et al., 2014).

Thus, structural and management practices aimed at decreasing CSOs are now considered to be unavoidable in lake restoration strategies (Huang et al., 2007; Watson et al., 2016), with huge costs to remove nutrients from point sources and implement related policies (e.g., Pretty et al., 2003). These costs are however far lower than the overall externalities of an uncontrolled eutrophication.

Indeed, the efforts to decrease nutrient loads are now leading to better water quality in many lakes in the world, such as Lake Maggiore (Morabito and Manca, 2014), Lake Constance, (Müller, 1997), Lake Geneva (Rapin and Gerdeaux, 2013), Lakes Vättern in Sweden (Wilander and Persson, 2001) and the Great Lakes in North America. There, expensive structural works have been implemented to mitigate the effect of CSOs, such as the storage system in Milwaukee (four deep tunnels 90 m deep under the ground surface, with a total length of 31.2 km and a total capacity of 1.53 10^6 m^3, Razak and Christensen, 2001), and the Tunnel and Reservoir Plan in the metropolitan Chicago area (e.g., Farnan et al., 2004). Considering a subset of 200 lakes originally included in a 1972-1976 National Eutrophication Survey, the U.S. Environmental Protection Agency (USEPA), 2009 concluded that 50% of the lakes exhibited an improvement in phosphorus concentration with respect to the 1972 survey. A holistic approach, relying both on measurements and modelling (maybe hybrid, *i.e.* mixing deterministic and stochastic models, as suggested by Obropta and Kardos, 2007), and investigating the functional relation between a lake and the surrounding sewer (Marsalek and Chocat, 2002; Moore et al., 2003), is fundamental to provide reliable estimates of the loads delivered by CSOs and of the actual effectiveness of the structural practices that must be adopted to improve water quality (Liu et al., 2014; Dai et al., 2016; Bravo et al., 2017; Chen et al., 2018). Following this approach, the main objective of this paper is to provide a comprehensive evaluation of the overall efficiency of the CSS along the eastern Lake Iseo shoreline, by combining the results of a monitoring campaign and of hydraulic modelling. The assessment of critical issues affecting the CSS is considered to be an unavoidable step before planning a long-term mitigation strategy to diminish CSO impacts on Lake Iseo. Lake Iseo, the fifth Italian lake in terms of volume, is an originally oligothropic (Bonomi and Gerletti, 1967) deep subalpine lake that has undergone a progressive quality degradation. Following a path common to several others lakes, over the last 50 years the strong nutrient load to the lake, originating from a large urbanized mountain catchment, and the growing density stratification reinforced by climate change (Valerio et al., 2015), has caused anoxia between 100 and 256 m depth. In this lake, after the construction of a main collector along the shoreline in 2000, the actual residual P load of CSOs has not been monitored. In order to evaluate the role of CSOs and the actual amount of nutrient loads discharged into the lake, two combined sewer weirs (CSWs) were monitored, one at the outlet of a tributary (or “municipal”) sub-catchment and the other at the outlet of the main diversion pipe, immediately upstream of the WWTP. At these sites, an extensive real-time monitoring campaign provided time series of the flow discharges and sewage samples during CSOs. The measured information on the CSOs frequency and on the amount of discharged Total Phosphorous (TP) and Total Nitrogen (TN), also documented the different dynamics of the first flush phenomena at the two sites.

In order to understand the hydrologic and hydraulic behavior of the network and to extrapolate the measured information to a longer 10 year period, for which a locally measured rainfall time series is available, a hydraulic model was implemented and calibrated by using the commercial software PC-SWMM (https://www.pcswmm.com/), that implements the well-known EPA SWMM5 capabilities within a user-friendly interface. The most important outcome of this computation was the statistical quantification of the residual nutrient loads discharged into the lake from the overall set of CSWs present in the modeled network. Furthermore, the observed rainfall time series was modified in order to account for a potential climate change scenario, developed according to expected climatic projections for this region. Thus, the calibrated model provided additional insight into the expected future variation of the CSOs volumes and nutrient loads.

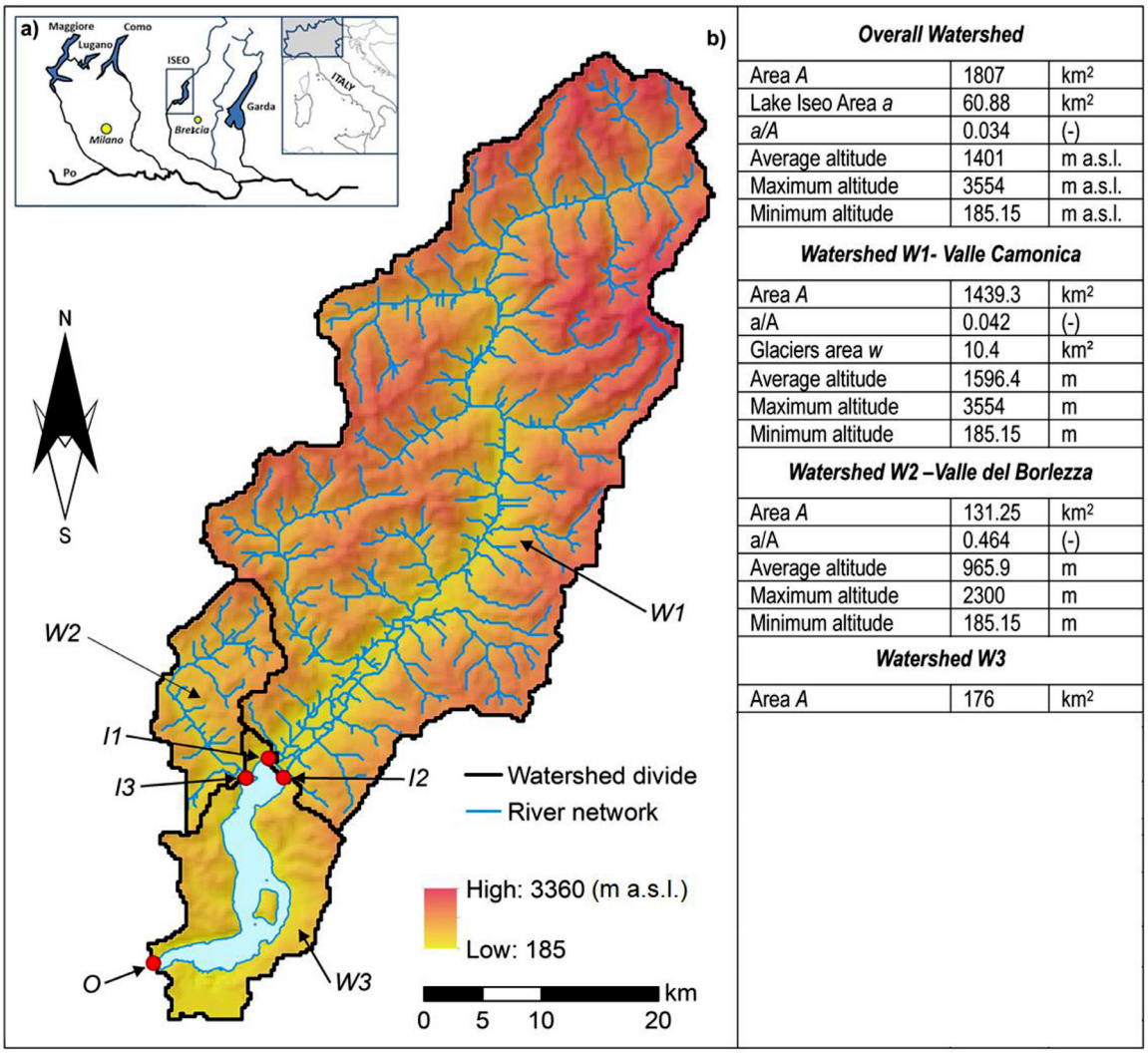

Overall Watershed		
Area *A*	1807	km²
Lake Iseo Area *a*	60.88	km²
a/A	0.034	(-)
Average altitude	1401	m a.s.l.
Maximum altitude	3554	m a.s.l.
Minimum altitude	185.15	m a.s.l.
Watershed W1- Valle Camonica		
Area *A*	1439.3	km²
a/A	0.042	(-)
Glaciers area *w*	10.4	km²
Average altitude	1596.4	m
Maximum altitude	3554	m
Minimum altitude	185.15	m
Watershed W2 –Valle del Borlezza		
Area *A*	131.25	km²
a/A	0.464	(-)
Average altitude	965.9	m
Maximum altitude	2300	m
Minimum altitude	185.15	m
Watershed W3		
Area *A*	176	km²

Fig. 1. a) Location of the study area in northern Italy and b) Lake Iseo within its watershed: *I1* (Oglio), *I2* (Canale industriale) and *I3* (Borlezza) are the main tributaries and *O* is the location of the dam in Sarnico.

The results of these detailed monitorings and modeling activities provided a clear view of the overall dynamics of the CSS and of the role played by the infiltration waters and led to propose an effective set of structural and non-structural practices to mitigate the environmental impact on the lake.

2. Methods

In this section the studied area is presented, along with the experimental campaign and modeling methods.

2.1. Description of the study area

Lake Iseo is a 256 m deep prealpine lake with a volume of about 7.9 10^9 m^3. It drains a 1807 km^2 mountain watershed (see Fig. 1) with a pollution load of about 1.9 10^5 population equivalent, characterized by 22% agricultural and 2% residential land use. The lake and the surrounding area are an important economic and touristic resource of northern Italy, to the point that in 2016 it was the location of a renowned artistic *en-plain air* performance, *The Floating Piers*, by the American artist Christo, where temporary orange walkways were set directly on the surface of the lake, which drew 1.2 million visitors (see Fig. 2).

In addition to the lake area (61 km^2), the lake watershed is mostly made up of two large valleys (Valle Camonica, 1440 km^2 and Valle Borlezza, 131 km^2, W1 and W2 in Fig. 1), and by a set of smaller watersheds that surround the lake (W3 in Fig. 1, 176 km^2). Accordingly, the lake area is only 3.4% of the drained area. According to the first limnological survey by Bonomi and Gerletti (1967), the lake was originally oligotrophic and well oxygenated even on the bottom. However, during the second half of the 20th century the lake underwent a dramatic water quality deterioration (e.g., Garibaldi et al., 1999). On the basis of our 2018 field measurements, water under 100 m (41% of the lake's volume) is anoxic with 102 µg/L of average total phosphorous. Moreover, the nutrient loads to the lake from the large drained watershed have contributed to a chemical stratification that hinders the mixing of the lake and makes the water renewal time longer with respect to its theoretical value. Recent studies prospect an increase in the thermal stratification in a climate-change scenario (Pilotti et al., 2014; Valerio et al., 2015).

The water level of Lake Iseo is regulated by a dam in Sarnico (point O in Fig. 1) and can vary between +110 cm and -30 cm with respect to the average value of 185.15 m above sea level, storing a volume of about 85 million cubic meters, mostly for agricultural purposes in the wide watershed downstream of the dam.

Fig. 2. Lake Iseo, near Monte Isola, during the Floating Piers artwork.

2.2. Description of the combined sewer around the lake

Both Valle Camonica (catchment W1 in Fig. 1) and Valle Borlezza (W2) have their own sewer systems and their waste waters drain into the most important lake tributaries (Oglio River, Canale Industriale and Borlezza River, see points I1, I2 and I3 in Fig. 1). Such systems will not be considered in this paper, since we focused our attention on the contribution from watershed W3, that is directly drained by the lake. The sewer system around Lake Iseo (catchment W3) is composed of two main sewers: the first sewer is along the western side of the lake ("Bergamo sewer", or BGS in the following), whose waste waters flow partly to a WWTP in Costa Volpino (WWTP2 in Fig. 3) and partly to a second WWTP in Paratico (WWTP1 in Fig. 3). The second sewer is placed along the eastern side of the lake ("Brescia sewer" or BSS in the following), whose waste waters flow to WWTP1 only.

The overall relevance and performance of the two sewers are comparable (about 36,000 population equivalent each), where both the east and the west coasts are characterized by similar morphologies and settlements. Thus, in the following, we will consider the Brescia sewer only, due to lack of data regarding the western sewer, and the conclusions obtained in the simulation of the BSS will be extended to the BGS.

The BSS is made up of a main collector with an overall length of 23 km (black solid line in Fig. 4) in which 9 tributary (or "municipal") sewers converge (grey solid lines in Fig. 4), for a total length of 257 km, mostly built with circular pipes with a diameter between 250 mm and 1600 mm. The main collector follows the lake shoreline and is made of polyethylene, reinforced concrete and spheroidal cast iron. Due to the small available topographic slopes, 12 pumping stations are present (green dots in Fig. 3) so that 17% of the conduits length is made up of pressurized delivery pipes and the remaining 83% is made up of free surface closed conduits with a slope between 0.1% to 1.5%. The main collector longitudinal profile is shown in Fig. 5.

All the 9 tributary CSSs converge into the main collector: for instance, the tributary CSS of the main lake island (Monte Isola) underpasses the lake and enters the pumping station S8. Actually, there are 51 junctions between the 9 tributary sewers and the main collector and 23 are characterized by the presence of a CSW (see red and pink arrows in Fig. 3), that during wet weather discharges the mixed sewage excess into the stream network drained by Lake Iseo. In addition, all the pumping stations except for S2 are provided with spill-over conduits, that are operated during maintenance or during very intense storms: these conduits discharge the CSO into the lake at a depth between 20 and 40 m. Finally, two CSWs are located along the main collector (see Fig. 3).

In the vicinity of the terminal pumping station (S1 in Fig. 3) the wastewater from BGS and BSS converge in a tank and the overall wastewater is pumped to the WWTP1 through two pressurized delivery pipes. Under the current operative rule, during intense storms the outlet of BSS in the tank is under pressure. Accordingly, in this circumstance the hydraulic behavior of the final part of BSS is influenced by the backwater caused by the tank water level, thus triggering the activation of the CSW in Paratico (Fig. 4) also for discharges lower than the design threshold.

The settlements drained by BSS amount to 12.8 km^2, but 31% of the area is drained by separated sewers, and the actual area that generates runoff is equal to 8.9 km^2. The overall impervious area drained by the BSS was computed by a suitable post-processing (Barone et al., 2019) of a recent Sentinel 2 satellite image obtained from Copernicus (https://scihub.copernicus.eu/dhus/#/home), with 10 m spatial resolution (see Fig. 6). The land use classification was based on the elaboration of a multi-spectral image in order to divide the watershed in land cover classes (water, built-up, vegetation and bare soil). The Sentinel 2 image includes the following bands: blue, green, red, near-infrared, short wavelength infrared 1 and short wavelength infrared 2. A land use class is assigned to each pixel based on the color band it belongs to.

The analysis was performed through the use of an open source QGIS plugin (Semi-Automatic Classification Plugin, SCP) that provides a set of intertwined tools for faster processing in order to create an automatic workflow to obtain

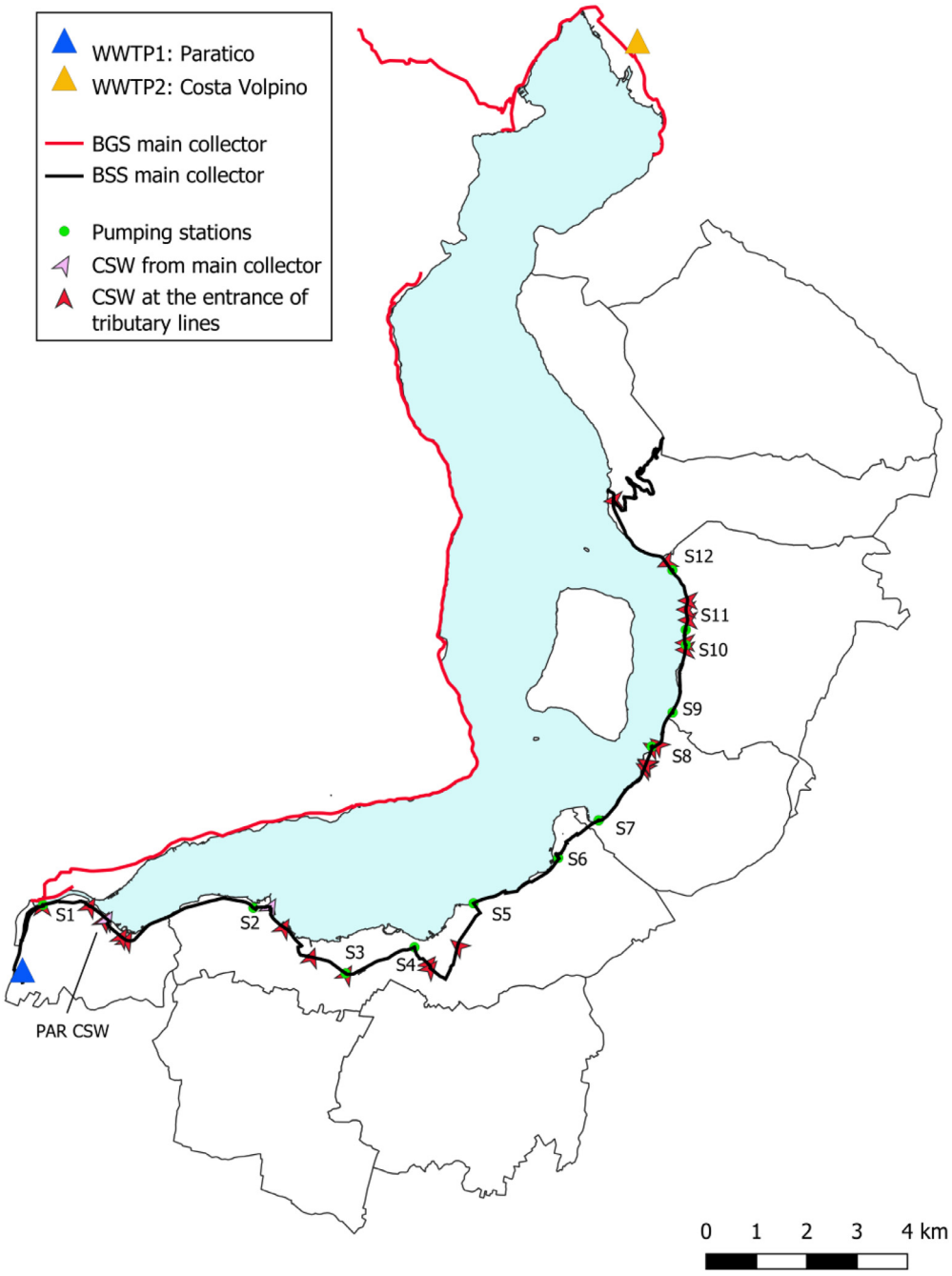

Fig. 3. Details of the BSS (black solid line) and BGS (red solid line) main collectors with the location of the pumping stations, overflow weirs and wastewater treatment plants for BSS.

land cover classification (see also https://readthedocs.org/projects/semiautomaticclassificationmanual/downloads/pdf/latest/).

The minimum surface that can be detected (100 m^2) can hinder the classification in pixels with a mixture of covers (soil, vegetation, …). However, this issue is counterbalanced by the large extension that can be easily mapped. Accordingly, in order to test the quality of the accomplished classification and to check that impervious areas were not erroneously classified (e.g., Pena-Regueiro et al., 2020), a visual validation was made for the Provaglio village using a box-counting approach on a high spatial resolution image of two typical neighborhoods with high and medium density built areas. The comparison with the visually recognised land use shows that the algorithm provides an excellent classification of the percentage of built areas in the high-density neighborhood (e.g., 86% versus counted 89% in the area A of Fig. 6) and, due to the typical dimension of house gardens and streets in the medium density neighborhood, tends to group them together as bare soils with a slight overestimation (e.g., 78% versus counted 61% in the area B of Fig. 6). Eventually, the overall computed impervious area was 3.0 km^2, i.e., 34% of the overall generating runoff area.

2.3. Detection of infiltrating waters along the combined sewer

By controlling the groundwater level along the shoreline, the variation of the lake water level over the year has important impli-

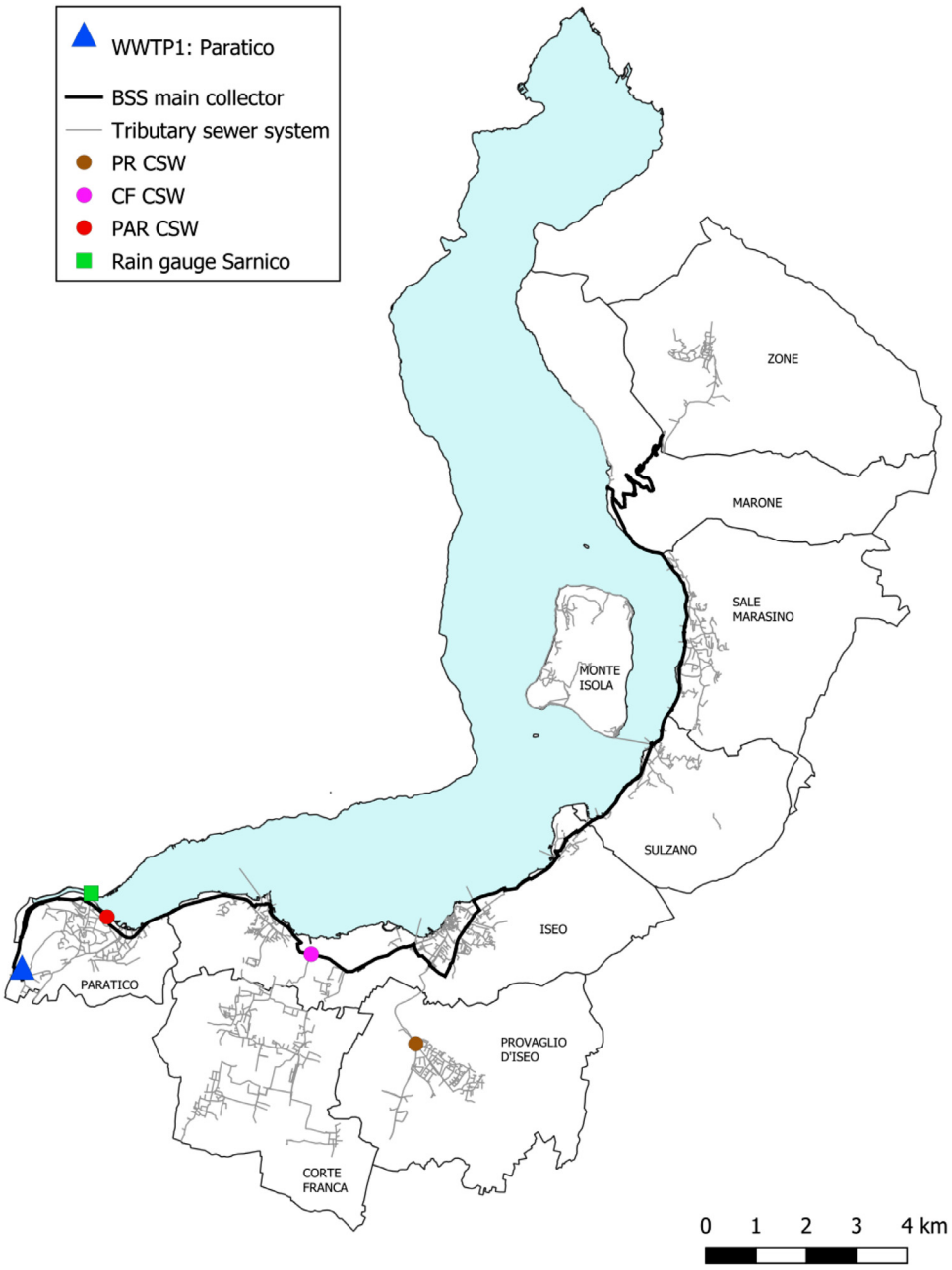

Fig. 4. Main collector (black solid line), tributary networks (grey lines), monitored CSWs: Corte Franca CSW (pink dot), Provaglio d'Iseo CSW (brown dot) and Paratico CSW (red dot), Sarnico rain gauge (square green dot) and Paratico WWTP (blue triangle dot).

cations on the functioning of the BSS. As shown in Fig. 5, a growing length of the main collector is under the elevation of the lake waters when the lake level increases. The percentage of the main sewage length below the lake water elevation varies linearly between 12% (minimum lake level) and 34% (maximum lake level). Due to the presence of leakage in the pipes, the higher the water level, the greater the groundwater infiltration within the sewer is. Potentially, also a moderate exfiltration into the groundwater could be expected when the lake level is very low, likely contributing to the contamination of the urban aquatic environment, but it will not be considered in the following.

The infiltration of groundwater into the BSS is clearly evident in the average daily flow discharges measured at the outlet in 2016, shown in Fig. 7 along with the lake level. As one can observe, there is a strong correlation between the two series: when the lake level grows higher than 50 cm (with respect to the conventional reference level) for a sufficiently long period of time, the baseflow follows a similar increase.

In turn, the groundwater infiltration in the sewer conduits causes discharges exceeding the design value of the pipes, with overflows from CSW also in dry weather periods, and a decrease in the sewage concentrations, with consequent issues in the functioning of the WWTPs. Accordingly, the identification of the actual stretches where leakage occurs is of paramount importance but is not an easy task in such a long network.

Different approaches can be used to assess the infiltration contribution to the flow discharge, namely the night minima observation, the flow volume balance (Staufer et al., 2012) and the isotope mass balance (Houhou et al., 2010). In this work, we adopted the second approach. By measuring the discharge at the end points of

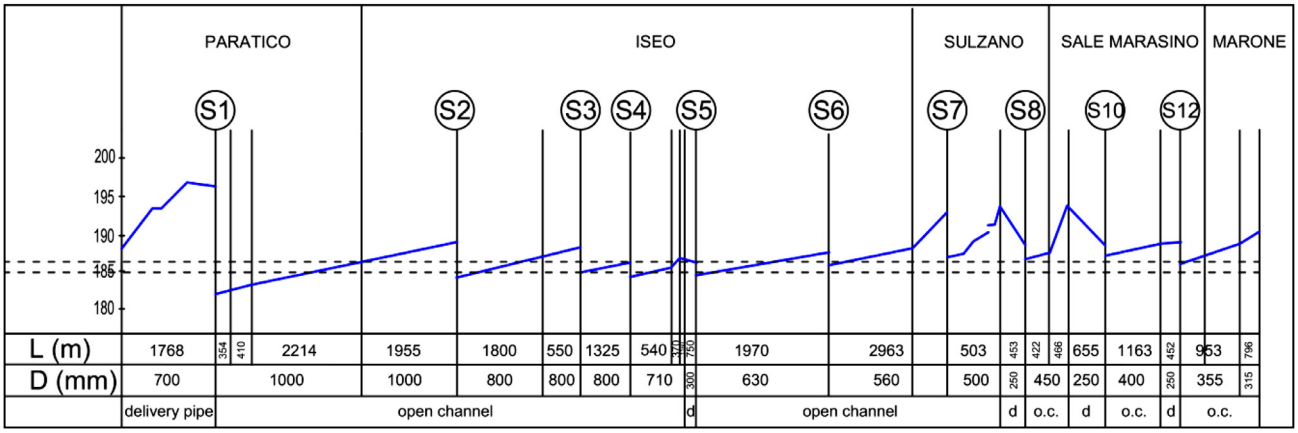

Fig. 5. Schematic view of the profile of the BSS main sewer; the dashed lines show the variation range of the lake level during the year and the encircled symbols are the pumping stations.

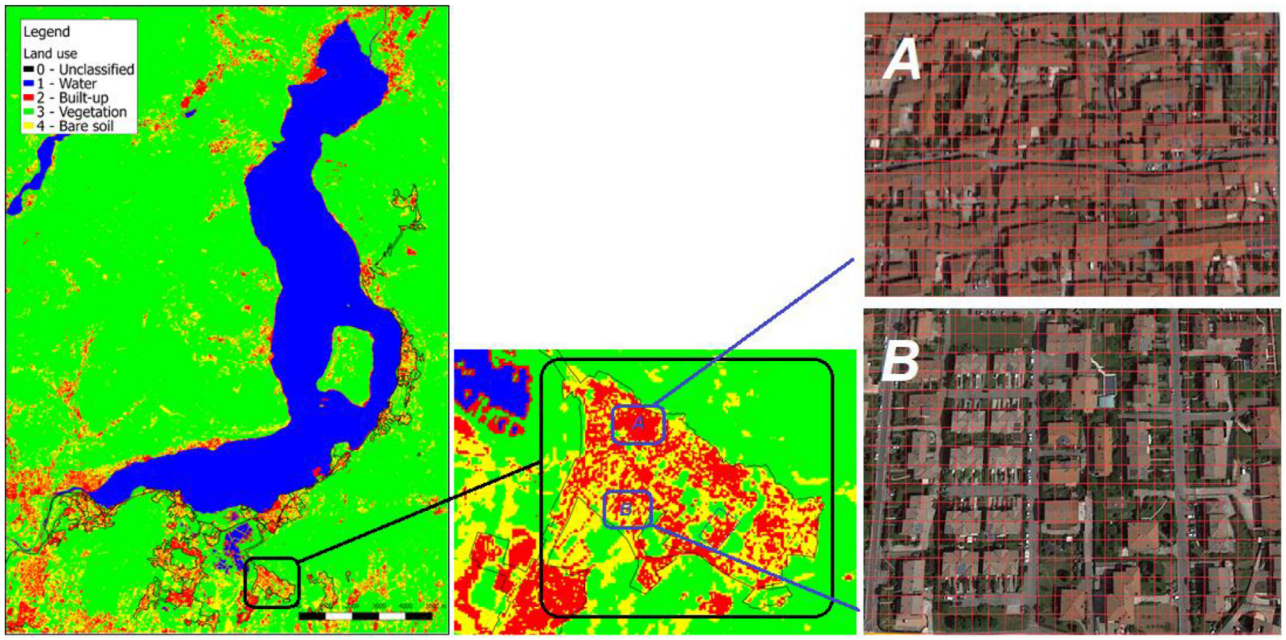

Fig. 6. On the left, land use classification by analysis of Sentinel 2 satellite images (resolution 10 m). Inset A and B show a comparison between the automatically classified land use and the prototype within a high density (A) and a medium-density (B) built neighborhood in the village of Provaglio d'Iseo.

a stretch during dry periods, when the storm water component is absent, and by knowing what discharges should enter the stretch along its extension (proportional to the drained population equivalent), one can compute the difference that can be reckoned as groundwater/lake infiltrations. From a practical point of view, since a flowmeter was not available within the sewer system until 2016, the task was carried out by analysing the sewage volume delivered at the pumping stations, in correspondence of different lake levels. In 2016 a flowmeter was installed immediately upstream of the terminal pumping station S1, confirming the value of the computed total infiltration for different stages of the lake. The analysis of the data until 2016 provides an experimental curve (see Fig. 8) of the overall infiltration as a function of the lake level. Quite interestingly, these data can be well approximated by a conceptual model for an orifice flow, as indicated in Eq. (1):

$$q = \begin{cases} C \int_0^L p \Delta Y^{0.5} dx & Y_{lake} > Y_{conduit} \\ 0 & Y_{lake} \le Y_{conduit} \end{cases} \quad (1)$$

where p is the local perimeter of the conduit exposed to infiltrations, L is its length, C is a constant and ΔY is the difference between the elevation of the lake (Y_{lake}) and the local elevation of the invert of the conduit ($Y_{conduit}$). If one regards the C coefficient as in Eq. (2):

$$C = \sqrt{2g} \cdot k \quad (2)$$

then an equivalent sewer porosity k could be introduced as a dimensionless measure of the relevance of the infiltration process in a sewer.

2.4. Available data and field measurements

All the geometrical and hydraulic information on the main sewer system (planimetric and altimetric layout of the network, lengths, diameters, materials, slopes, location and types of spillways) were provided by the drainage network manager (Acque Bresciane). The pumping stations were characterized by their geometry, the operative rules and the characteristic curves of the pumps.

Table 1 shows the temporal availability of the measured time series. The lake level and the rainfall series with a time step of 10

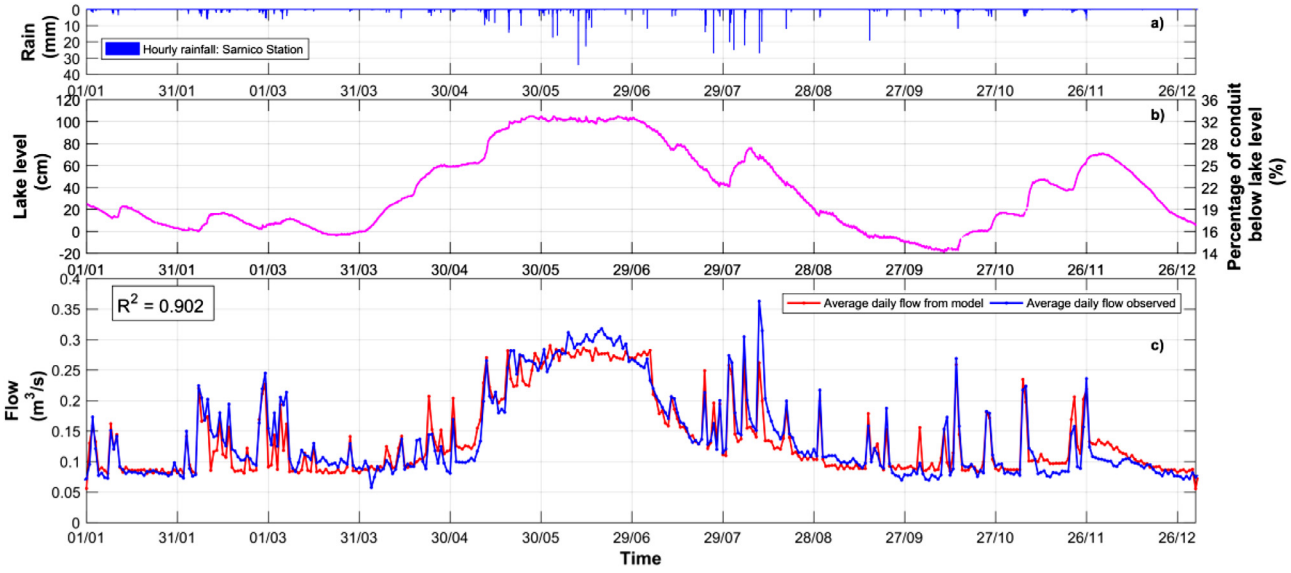

Fig. 7. a) Hourly rainfall depths observed at Sarnico raingauge by ARPA Lombardia, b) daily Lake Iseo levels and c) comparison between measured and modelled average daily flow discharges at the pipe outlet for the year 2016.

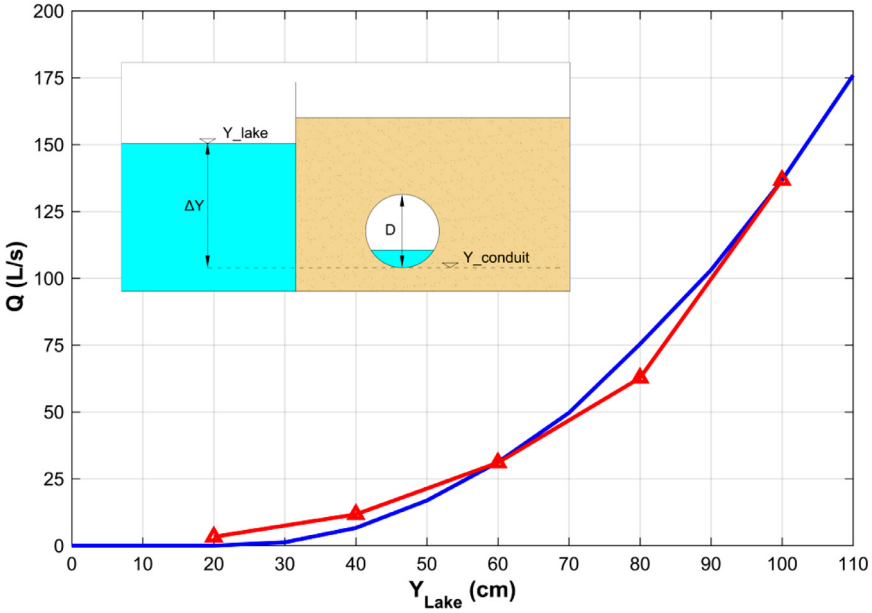

Fig. 8. Comparison between infiltration discharges Q obtained by the operation times of pumping stations (red triangles) and by the proposed infiltration model (blue solid line) in the downstream part of the main collector.

minutes for the Sarnico raingauge were available for a 10 year period (source: ARPA Lombardia). With regard to the discharges, the ones pumped by the eight pumping stations were available for a 7 month-long period in the first half of 2015. At the end of the collector, two data sets were available: the discharge that has entered WWT1 since 2015, obtained by the operation time of the pumps at the pumping station S1 in Paratico, and the one measured since August 2015 by Acque Bresciane at the final station of the main collector, using an area-velocity flowmeter (Nivus PCM 4) with an error $< 0.5\%$ of measurement $+5$ mm/s when $v < 1$ m/s and $< 1\%$ of measurement when $v > 1$ m/s.

Accordingly, the overall discharge of the main collector is available from 2015 with a time step of 5 min and was used, along with the rainfall, for the model calibration. The discharge entering from the BGS main collector was computed as a difference between flow discharges measured in correspondence of WWTP1 and the flow measured at the outlet of the BSS main collector.

In order to study the frequency and the quality characteristics of the COSs from the CSWs existing in the whole network, we monitored two different CSWs: the first, representative of overflows from the tributary sewers, is located upstream of the junction of the Corte Franca sewer with the main collector (see CF CSW in Fig. 4). The second, representative of overflows from the main collector, is located at Paratico (see PAR CSW in Fig. 4). Indeed, one can expect differences in the quality of the two overflows since the main collector is characterized by a longer residence time, stronger mixing and dilution with infiltrating waters. In both cases the flow discharge was measured and sewage samples collected automatically with a portable sampler during CSO occurrences. The extensive monitoring campaign at the CF CSW is described in detail in Barone et al. (2019). On the other hand, the quality of the water

Table 1
Available time series of measured data and corresponding periods (* first half-year, + second half-year).

	2007	2008	2009	2010	2011	2012	2013	2014	2015	2016	2017	2018
Time of operation of pumping stations									X*			
Lake Iseo levels	X	X	X	X	X	X	X	X	X	X	X	X*
Rainfall series (Sarnico station)	X	X	X	X	X	X	X	X	X	X	X	X*
Discharge in PS1 from BS main sewer system									X+	X	X	X*
Flow entering the WWTP from BS and BG									X	X	X	X*
Overflow discharge series in PAR CSW											X+	X*
Overflow discharge series in CF CSW											X+	X*
Overflow discharge series in PR CSW											X+	X*

Table 2
Dates of monitored CSO events of PAR CSW, parameters analysed in laboratory and number of samples for each event; main characteristics of the rainfall events triggering the monitored CSOs and corresponding quality parameters: antecedent dry weather period a, wet weather duration d, rainfall depth h, maximum rainfall intensity i_{max}, event mean concentration EMC and exponent b of the DCL curves for TN and TP, and summary statistics of quality parameters.

Event	Event start date	Event end date	Samples nr	Parameters analysed					a	d	h	i_{max}	EMC (mg/L)		b	
	dd/mm/yyyy hh:mm	dd/mm/yyyy hh:mm		TN	TP	COD	BOD_5	TSS	(h)	(h)	(mm)	(mm/h)	TN	TP	TN	TP
1	04/04/2018 00:00	04/04/2018 06:50	5	x	x	x			375.5	4.8	7.6	2.4	29.5	4.1	1.00	0.99
2	10/04/2018 00:10	10/04/2018 03:10	9	x	x	x			121.3	1.5	7.8	13.2	27.4	5.1	0.90	0.92
3	11/04/2018 20:10	12/04/2018 12:00	18	x	x				23.2	6.2	13.6	10.8	8.7	1.2	0.70	0.72
4	30/04/2018 00:00	30/04/2018 05:50	16	x	x				397.0	2.3	5.4	4.8	22.5	3.8	0.86	0.85
5	09/05/2018 17:30	09/05/2018 23:30	19	x	x				15.3	1.8	6.2	12.0	16.0	1.9	0.85	0.94
6	16/05/2018 21:40	17/05/2018 04:20	18	x	x				45.0	4.5	9.0	4.8	17.0	2.2	0.98	1.04
7	23/05/2018 17:40	23/05/2018 22:40	6	x	x				157.5	0.7	7.6	27.6	22.6	3.3	1.15	1.27
8	04/06/2018 07:30	04/06/2018 23:20	6	x	x	x	x	x	138.7	2.8	29.6	50.4	10.8	1.5	0.78	0.78
9	12/06/2018 09:00	12/06/2018 11:50	5	x	x	x	x	x	56.3	0.7	1.6	6.0	9.7	1.4	1.03	1.09
10	03/07/2018 21:30	04/07/2018 00:40	5	x	x	x	x		369.3	3.0	7.2	6.0	30.9	5.0	0.88	0.94
Mean													19.5	3.0	0.91	0.96
Minimum													8.7	1.2	0.70	0.72
Maximum													30.9	5.1	1.15	1.27
Variation coefficient													0.43	0.51	0.14	0.17

overflowing from the CSW along the main collector is crucial, because at each pumping station, an overflow pipe exists that during intense storms discharges waters directly into the lake under the thermocline. Accordingly, the monitoring of PAR CSW is representative of this second category of CSOs. From May 2017 at the PAR CSW a level sensor LT-US Lacroix Sofrel was installed (accuracy within the maximum between 6 mm and 0.25% of the measured range) by which the discharged flow series was computed.

In April 2018 we also installed an automatic sampler ISCO 3700 equipped with 24 ½-liter bottles, to collect CSO samples. The sampling interval was set equal to 10 minutes and the sampler was set up to collect two samples of 250 mL in each bottle, in order to characterize the overflowing sewage during 8-hour long events. Within a few hours after collection, the samples were transported using a portable refrigerator to the laboratory to quantify TP and TN concentrations. Overall, a total of 10 CSO events and 107 samples were analyzed. Unfiltered water samples were analyzed for TP and TN concentrations with standard spectrophotometric (Perkin Elmer, Lambda 35) methods as soluble reactive phosphorus and nitrate after alkaline peroxydisulfate oxidation (Valderrama, 1981). In some cases, the laboratory also carried out analysis of Chemical Oxygen Demand (COD, 5 events, APHA, 2012), Biochemical Oxygen Demand at 5 days (BOD5, 3 events, UNI EN 1899-1 2001) and Total Suspended Solids TSS (2 events, APAT CNR IRSA 2090 B Man 2003). Considering that only accurate analytical results allow valid conclusions to be drawn, in Appendix 1 further information is provided regarding the quality assurance and quality control followed in the measurement of chemical data.

The dates of CSO events when the stormwater runoff samples were collected are summarized in Table 2, along with the parameters analyzed in laboratory and the numbers of samples for each event. During these events, the CSO discharge was measured, as well.

2.5. Hydraulic-hydrological model

The combined sewer was modeled using the Storm Water Management Model (SWMM) developed by the United States Environmental Protection Agency, operating within the PCSWMM environment. This software computes both surface runoff and flow in conduits, using hydrological, hydraulics and geometrical characteristics of the watershed and the sewer network (e.g., Gironás et al., 2010; Rossman, 2015). Although SWMM allows researchers to study water quality, we limited our use to the reproduction of the sewer hydraulics.

Due to the complexity of the overall system and to the lack of adequate geometrical information on the whole set of the tributary sewers, we developed the hydraulic models of the main collector and of two tributary sewer systems only, namely Corte Franca and Provaglio d'Iseo (Fig. 4). Such tributary drainage systems were monitored at their outlet sections, immediately upstream of the confluence in the main sewer, by using a calibrated stage-discharge curve and level meter. Their calibration during wet-weather periods (Barone et al., 2019) provided the hydrological parameters of the corresponding watersheds, that were used for the lumped hydrological modelling of the other 7 similar tributary sewer systems. Considering that during intense storms, likely yielding CSOs, the decrease in the soil infiltration capacity in urban areas is negligible, a simple infiltration model featuring a constant infiltration rate f_P (mm/h) was used. In the totally impervious urban area f_P was set at 0 mm/h, whereas in the remaining pervious area it was set at 3 mm/h. The rainfall time series used as the model input was provided by the regional meteorological monitoring agency ARPA Lombardia for the rain gauge located in Sarnico (see Fig. 4). In this series, the rainfall depths were recorded every 10 minutes, a time step that can be considered sufficiently short with respect to the tributary sewer network response times. The computed discharges

delivered by the tributary sewers were used as external inflow discharges in the junction nodes of the main collector.

In addition to the geometrical characteristics of pipes and manholes, the functioning of the pumping stations placed along the main sewer was modeled in detail, by implementing the geometry of the storage tanks, the characteristic curves of the pumps, the geometrical data of the delivery pipes and the startup and shutoff depths of the pumps. The hydraulic characteristics of the different CSWs were also implemented in the model.

The dry weather loads were calculated by multiplying the daily per capita water supply (estimated in 250*0.8=200 L/(p.e.d), according to the data supplied by the company managing the tributary drinking water plants) by the population equivalent in the area of interest. This load was incremented considering the touristic seasonal loads (data provided by the national statistics institute ISTAT), so that a monthly time pattern was obtained for the dry weather flow. The hydraulic model also accounted for the infiltration waters, computed as a function of the lake levels according to Eq. (1). Calibration led to a value of 1.12 10^{-5} for the porosity coefficient k in Eq. (2). As can be seen in Fig. 8, the agreement between the measured and modeled infiltration water discharges is satisfactory. Fig. 8 also shows that when the lake level is at a maximum (i.e., +110 cm), the infiltration water contribution corresponds to 175 L/s, that is 150% of the normal waste water flow discharge in dry weather periods

Since the water depth in the S1 pumping station is influenced also by the flow discharge coming from BGS, its contribution had to be evaluated without the possibility of modelling its hydraulic behavior in detail. Therefore, during dry weather periods, we assumed an overall discharge proportional to the population equivalent in the BGS drained area. Conversely, during wet weather periods, we introduced a fictitious subcatchment whose runoff directly enters PS1. This subcatchment model was calibrated by using data from 2016, on the basis of the difference between the overall discharge measured at the WWTP1 and at the BSS outlet. The calibration of the BSS main collector was instead limited to the choice of the friction factors on the basis of the typical pipe materials.

3. Sensitivity to climate change

Considering that the rainfall-runoff transformation is a strongly non-linear process, affected by the infiltration excess of rainfall, one can expect that an increase in the rainfall intensity, as a likely outcome of the ongoing climate change, could lead to a worsening of the environmental impact of a combined sewer due to the increase in the frequency and volume of CSO events (e.g., Nie et al., 2009; Fortier and Mailhot, 2015; Semadeni-Davies et al., 2008). Considering the "*business-as-usual*" emission scenario RCP8.5 (IPCC, 2014), Sinha et al. (2017) have shown that climate change–induced precipitation changes alone will substantially increase (19 ± 14%) riverine total nitrogen loading within the continental United States, fostering further eutrophication. Unfortunately, this scenario, referring to the worst greenhouse gasses emission projection, currently appears to be the most probable one, with respect to the RCP4.5 "*stabilization*" scenario and to the RCP2.6 "*mitigation*" scenario.

To evaluate the consequences of this scenario on CSOs with reference to 2100, Salerno et al. (2018) proposed an increase in the rainfall intensity of 20%, dealing with a case study located in this climatic region. Actually, in northern Italy, statistically significant increases in the yearly total amount of precipitation are not expected. Conversely, seasonal trends should yield increases in the rainfall depths in summer and spring, along with decreases in winter and autumn. In particular, winter storms would be affected by a more complex change, according to which the mean should decrease and the upper percentile should increase; see, for instance, Balistrocchi and Grossi (2020) for a review. It is worth noticing that, the temporal structure of storms in northern Italy shows a significant seasonality, so that storms featuring short durations and high intensities mostly occur in late spring and in summer. Long frontal events with larger depths but low intensities are instead more common in the other seasons. Therefore, a reasonable scenario for the study area could involve an increase in heavy storms and a decrease in moderate and low intense rainfalls. In this study, this was accomplished by globally increasing the observed heavy storm events of 20% and by cutting the values under a threshold, calculated in order to keep the yearly cumulated rainfall constant.

4. Results and discussion

4.1. Model calibration and field data analysis

In this section we discuss the exploitation of the extensive data set, collected as illustrated in the previous section, to the characterization of the quantitative and qualitative aspects of the combined sewage.

4.1.1. Results of the hydraulic-hydrological model

Fig. 9 shows the comparison between modeled and measured flow discharges at the outlet of the BSS into PS1 and modeled and measured overflow discharges at PAR CSW, for the period 01/05/2017 – 04/05/2017. In consideration of the system complexity, the model reproduces the behavior of the Brescia main collector well. Fig. 10 shows additional comparison between the modeled flow discharge and the computed one from BGS and from BSS for the period 01/01/2016 – 14/01/2016.

The model was validated by using the Sarnico rainfall series during the entire year of 2016. The graph in Fig. 10 shows the comparison between simulated and measured daily average flow discharges coming from BSS. The satisfactory agreement between measured and modeled flow discharges shown in Fig. 10 is supported by a linear correlation coefficient of R^2=0.90. The strong influence of the lake water levels on the sewer flow discharges in the period 30/04 and 29/07 is also evident. Overall, the modeled network closely reproduced the measured discharges at the main collector outlet.

4.1.2. Quality data analysis of CSOs

The two flow discharge gauges and the two portable samplers installed in CF CSW and in PAR CSW provided fundamental data on the quantity and concentration of nutrients discharged into the lake. Due to the hydrologic and land-use similarity between the different small watersheds, the CF CSW is considered representative of overflows from the 9 watersheds drained by tributary lines: the 8 month activity at CF CSW during which 18 overflows were sampled was carefully documented in Barone et al. (2019). The most interesting results are the presence of a moderate-weak first flush, whose strength is significantly correlated with the duration of the antecedent dry-weather period, and the occurrence of frequent CSO events but with moderate volumes; this implies that a small water quality volume must be provided in order for a capture storage tank to be effective.

On the other hand, during the 4 month monitoring activity at the PAR CSW, a total of 10 events were observed, also representative of the overflows that characterize the main sewer at the pumping stations. The differences in the hydraulics of these two systems have remarkable consequences also on the quality of the discharged waters.

The thick solid line in Fig. 11 shows the linear regressions between TN concentrations and TP, BOD, COD and TSS in the individual sample bottles. The dashed line shows the same regressions as computed from the measured data at the CF CSW

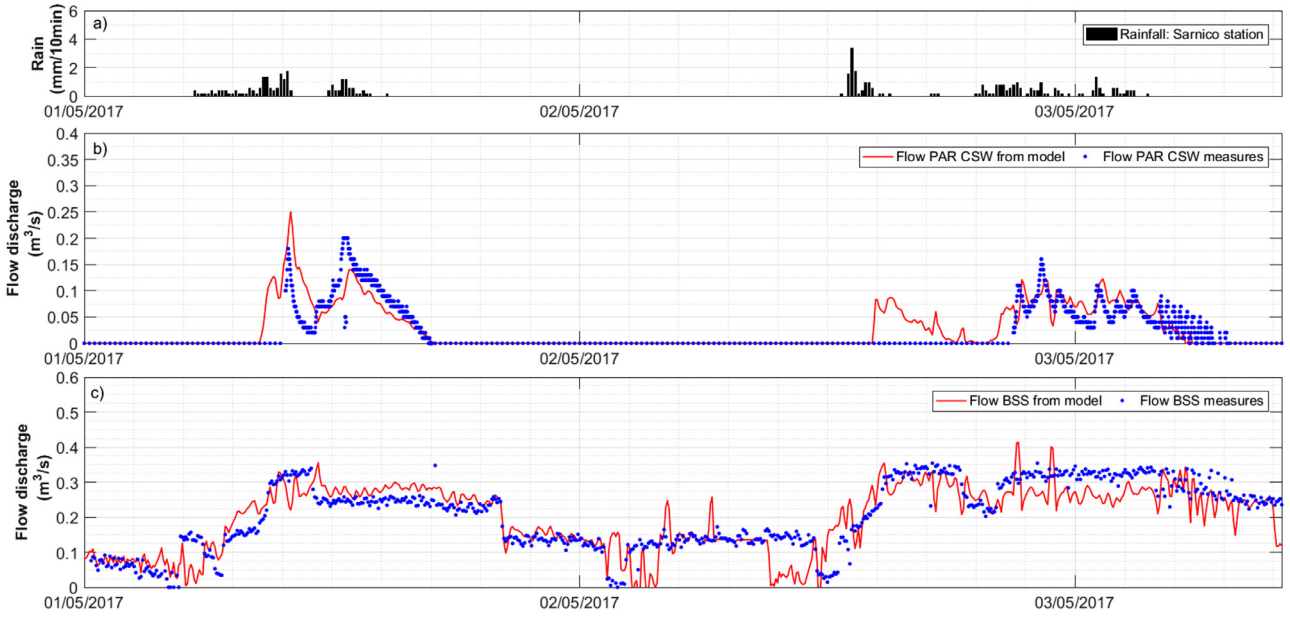

Fig. 9. a) Rainfall depths in Sarnico raingauge recorded at a time step of 10 minutes, b) comparison between modelled and measured flow discharges discharged from PAR CSW into the lake and c) entering PS1 from BSS plotted at a time step of 5 minutes.

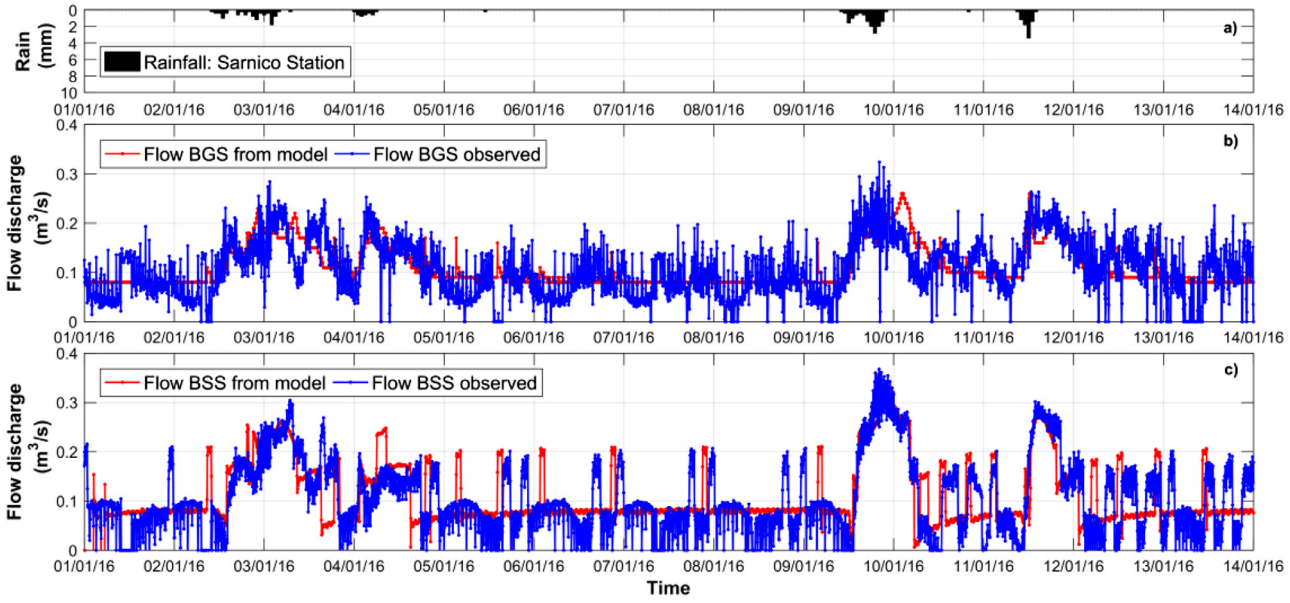

Fig. 10. a) Hourly rainfall depths in Sarnico station, b) comparison between modelled and measured flow discharges entering PS1 from western main collector (Bergamo province) and c) from eastern main collector (Brescia province) plotted at a time step of 5 minutes.

(Barone et al., 2019). As observed for the CF CSOs data, a significant linear correlation between TP and TN concentrations is observed. The TN/TP mass ratio is consistent with the expected range for civil sewage and with the one obtained for CF CSW (about 5). This strong correlation confirms the similarities between the TN and the TP transport dynamics in terms of event mean concentrations. Furthermore, good correlations are obtained also for the other three variables showing that, *inter alia*, a significant BOD removal takes place along the main sewer.

In order to investigate the occurrence of the phenomenon of first flush in CSOs from the main sewer, we decided to use the dimensionless diagrams of the nutrient load and discharge volume (dimensionless cumulative load – DCL- curves) proposed by Bertrand-Krajewski et al., 1998. Since the early studies on wet weather discharge quality (e.g. see the review by Deletic, 1998), the occurrence of first flush is an aspect of the pollutant delivery dynamic that continues to be debated (Sansalone and Cristina, 2004; Gnecco et al., 2005; Gikas and Tsihrintzis, 2012; Ekanayake et al., 2019). Its practical implications on the design of structural devices devoted to the mitigation of urban stormwater impacts are relevant (Baek et al., 2015; Mamoon et al., 2019). Indeed, issues regarding the factors affecting its occurrence are manifold and still deserve to be investigated and ranked (Francey et al., 2010; Frazar et al., 2019; Perera et al., 2019).

In DCL curves, ratio ν between the cumulative and total discharge volume is reported on the x axis and ratio λ between the cumulative pollution load and the total pollution load is reported on the y axis. The empirical DCL curves can suitably be fitted by the power function reported in Eq. (3) (Balistrocchi et al., 2009; Ma et al., 2011), where the exponent b measures the strength of

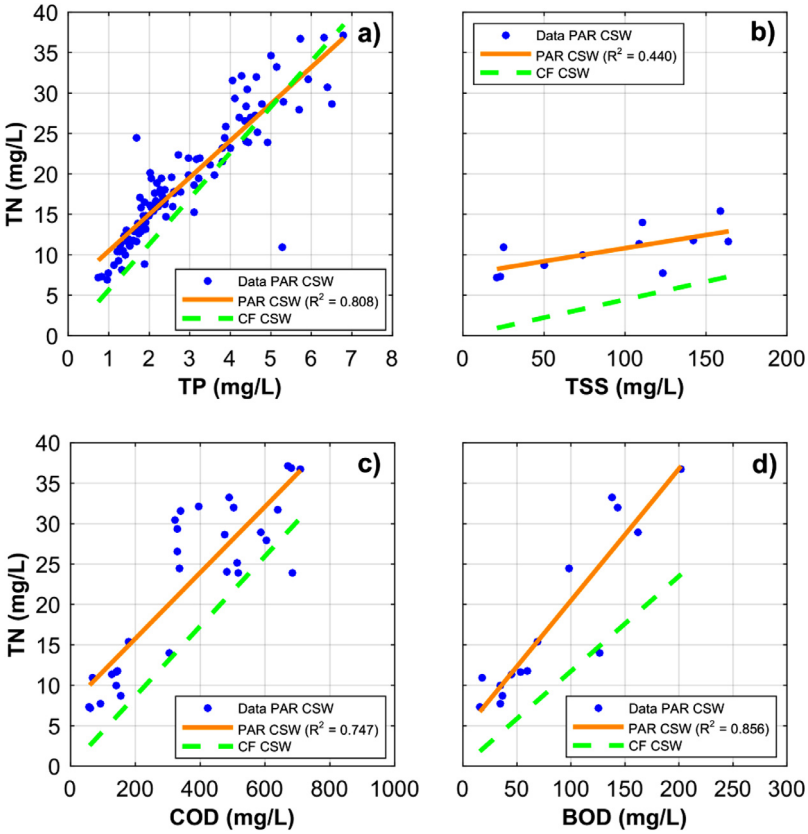

Fig. 11. Linear regressions between TP, TSS, COD, BOD concentrations and TN concentrations detected in the analyzed sample bottles for PAR CSW (orange solid lines) and comparison with the linear regressions obtained for CF CSW (green dashed lines).

the first flush.

$$\lambda = \nu^b \tag{3}$$

According to this formulation, the greater the first flush, the smaller the value of exponent b is, while a unitary value of exponent b shows the absence of the first flush. Alternative methodologies have actually been proposed to assess the existence and the intensity of the first flush after DCL curves. For instance, Bach et al. (2010) developed a method based on a cluster analysis which involves the separation of the flow volume into slides. However, the DCL curve approach has advantages in terms of practical applicability, computational intensity and uncertainty with respect to arbitrary choices of the analysis parameters.

The main characteristics of the monitored CSO events for the PAR CSW are shown in Table 2 where the rainfall events are delineated in terms of depth, duration, maximum intensity and antecedent dry weather periods, while the pollutant dynamic is summarized by the observed event mean concentrations (EMC) of TN and TP and exponent b of the power functions (3), fitted to the empirical DCL curves. Statistics of these quality parameters are reported, as well. The measured DCL curves for the PAR CSW are shown in Fig. 12, along with the average DCL curve. For the sake of comparison, also the average DCL curve for CF CSW is shown in the same Figure. Table 2 and Fig. 12 show that the average PAR DCL curve is characterized by a rather uniform concentration during the overflow (b close to 1.0). This result is in contrast to the case of CF CSW, where a moderate first flush is present (b close to 0.7 and 0.65 for TN and TP, see also Barone et al., 2019). This remarkable difference can partly be explained by groundwater infiltration that, however, due to its characteristic time, contributes in a similar way to the different parts of the pollutograph and in a negligible way in the case of low lake levels. More likely, the increased discharge due to infiltration waters prevents pollutant sedimentation during dry weather periods. The resuspension of dry weather sedimentations is broadly acknowledged as a leading cause for the first flush occurrence. A further explanation can be found by considering that CF CSW drains a single tributary network, whereas the flow entering the PAR CSW is the combination of several tributary network inputs distributed along the main sewer over more than 20 km. Tributary watersheds feature different stormwater delivery times. Therefore, in the main collector there is an overlapping of pollutographs characterized by different times to peak, decreasing the overall variability of the pollutant concentration. Finally, the action of the pumping stations certainly increases the pollutant mixing, thus contributing to a more uniform concentration during the event.

4.2. Long-term continuous simulations

The calibrated model of the main sewer network was used to perform a 10-year (from 2007 to 2016) continuous simulation by using the Sarnico rainfall series provided by ARPA Lombardia (time step: 10 minutes). Bearing in mind the eutrophication process of Lake Iseo, the fundamental result of the 10 year simulation is the quantification of the volume of waters discharged into the lake from the BSS during wet weather periods and the quantification of the corresponding pollutant load (residual load). However, there is a difference between the CSWs along the main collector and the ones at the end of the tributary sewers, because in the first case, due to the absence of the nutrient first flush, the pollutant load can simply be considered proportional to the discharged volumes.

Accordingly, in the following the overflows from the tributary CSWs (e.g., the CF CSW), where a first flush is present, were clustered as Type 1 overflows. On the other hand, the overflows occur-

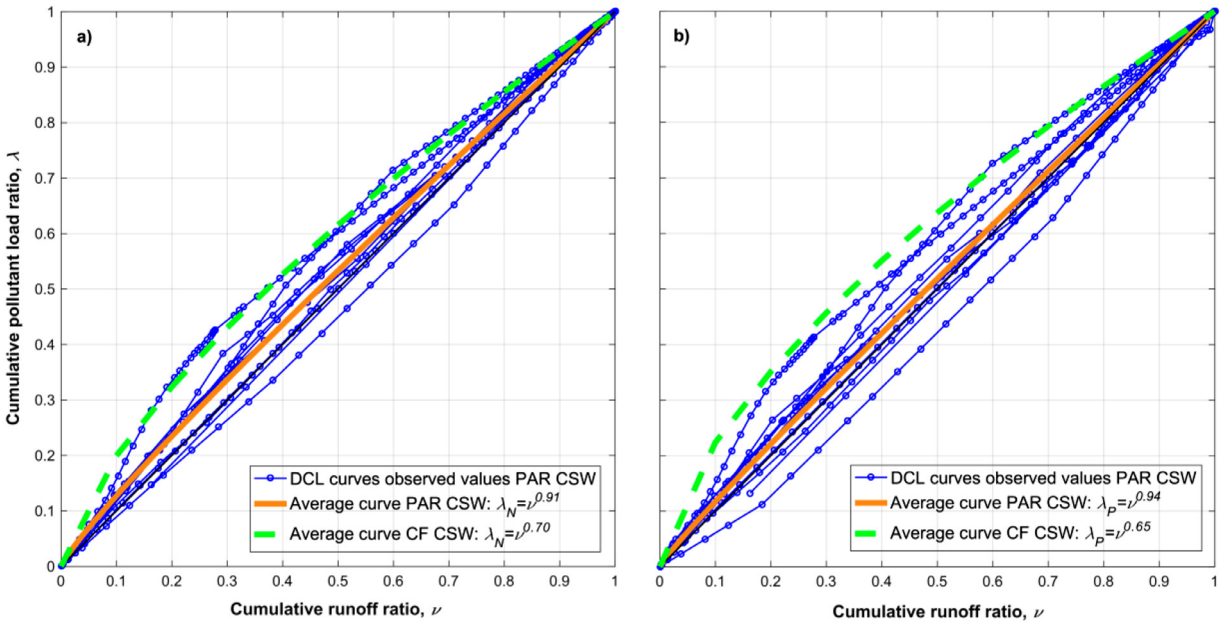

Fig. 12. Dimensionless cumulative load (DCL) curves observed at the monitored PAR CSW for a) TN and b) TP and comparison between the power functions approximating the average behaviours assessed for PAR CSW (orange solid lines) and CF CSW (green dashed lines).

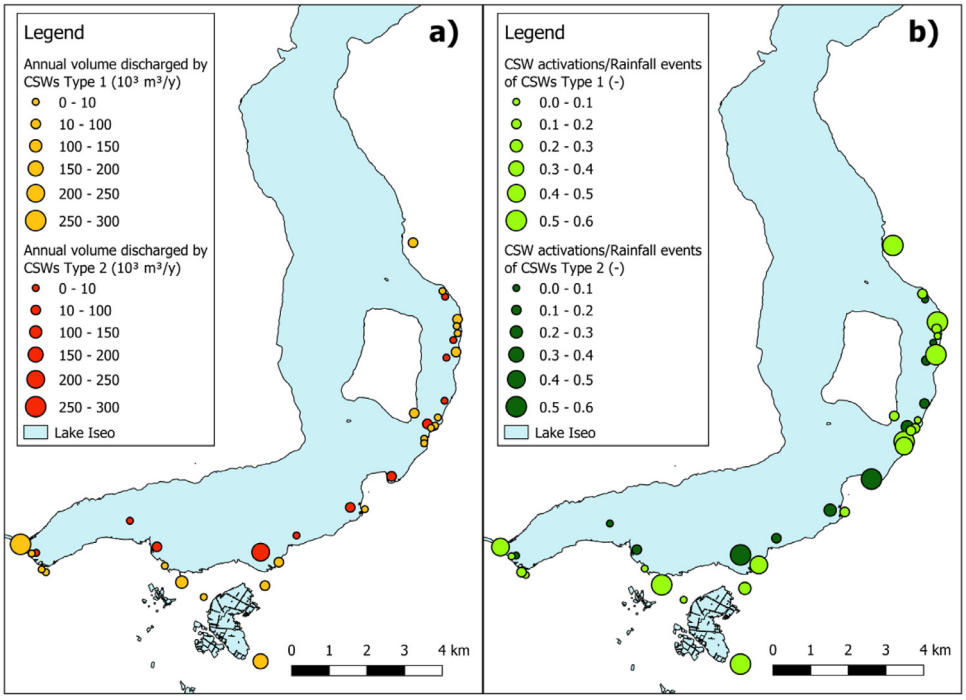

Fig. 13. a) Map of annual volumes discharged by CSWs Type 1 (final CSW of a tributary network) and CSWs Type 2 (overflows from the main collector) and b) map of the activation frequency of CSWs (number of CSOs events/number of rain events) individual overflow events are identified by using a minimum 3 hours inter-event time.

ring along the main collector (e.g., the PAR CSW or the overflows from the pumping stations), were clustered as Type 2 overflows.

Overall, during the 10-year period covered by the simulation, the CSWs Type 1 discharge amounts on average to 8.44 10^5 m^3/year and the CSWs Type 2 amounts to 3.66 10^5 m^3/year, for a total of 1.21 10^6 m^3/year. Considering that the sewage flowing towards the WWTP1 from the BSS is on average 5.16 10^6 m^3/year, the volumetric efficiency of the sewer, i.e. the percentage of volume that reaches the terminal wastewater treatment plant, with respect to the total volume entering the combined sewer system, is equal to 81%.

Fig. 13 reports the spatial distribution of the annual volume discharged by each CSW (panel a) along the BSS and the frequency of CSO events, defined as the ratio between the number of CSO events and the number of rainfall events (panel b). These maps are particularly important because they show the location of places were a localised environmental impact can be expected. They also show the frequency of these overflows during rainfall events, un-

derlining the threat that they pose to the touristic vocation of the lake.

An additional fundamental result of the long-term simulation is the average yearly residual load to the lake from the BSS, obtained by multiplying the volume discharged by CSWs Type 1 by the EMC of nutrients of CF CSW and the volume discharged by CSWs Type 2 by the EMC of nutrients of PAR CSW, obtaining 3445 kg of TP and 21758 kg of TN per year.

Considering that the BGS has similar characteristics to the BSS and that the population equivalent of the southern part of the BGS drained area is similar to the BSS one, it is possible to calculate the total contribution of BSS and BGS by doubling the previous results. It is more informative to see these figures in relative terms: considering a pollution load of 36000 population equivalent and the per capita water supply of 250*0.8 L/(p.e.d), by assuming typical literature concentration values for dry weather sewage (tipically in the range 6:10 mg/L for TP and 20:40 mg/L for TN), the average percentage of yearly loads discharged into the lake with respect to loads produced in the drained area is equal to 13.1%-21.8% for TP and to 20.7%-41.4% for TN. These values are largely dominated by the contribution from Type 1 CSW. It is here interesting to observe that these results are much larger than the ones adopted during the initial design of the main sewer around the lake, when the overall residual P load of CSOs was reckoned at about 3% of the overall load to the sewer (Garibaldi et al., 1997).

In the particular case of Lake Iseo, the computed value of about 7000 kg of overall residual TP from the CSOs of the 2 peripheral sewers are in the order of 6% of the TP load from the much larger watershed W1 (about 110 tonns/year, measured by an auto-analyser and by period sampling at mouth I1 and I2, Fig. 1, of the main tributaries; similar measures for TN are about 2100 tonns/year). From a different perspective, another indication of the relevance of the contribution can be provided by a “back of the envelope” evaluation of the admissible P load to the lake, according to the well-known Vollenweider (1975) model (also used in the 1982 OECD eutrophication modeling approach), who related the P load to a mean depth/hydraulic residence time ratio on a plot where two reference subjective curves, representing excessive and permissible loading, were represented. Considering that the theoretical renewal time of lake Iseo is about 4.3 years, its average depth is 130 m and its volume is 7.9 $10^9 m^3$, the excessive load would correspond to 61 tonns/year and the permissible one would correspond to 30. Accordingly, the residual load from CSOs would correspond to 22% of the overall permissible load.

In general, a residual TP contribution of 20% can be unbearable in a lake restoration project, also considering that CSOs are primary sources of microbiological contamination (e.g., Bryan Ellis and Yu, 1995) that may hinder bathing in the lake waters and the integrity of drinking water (Madoux-Humery et al., 2013) if a potential interaction between the influence areas of CSOs and major touristic areas or water intakes is present. Finally, the strong nutrient inflow in localized spots along the shore cause an impairment of the habitat: Ghirardi et al. (2019) highlighted the presence of the peculiar phenomenon of the submerged aquatic vegetation uprooting, that is related to an excessive organic matter accumulation in sediments, just in front of the CF CSW, whose overflows significantly contribute to the nutrient pollution of this littoral area.

It is well known that deep lakes will greatly suffer climate change mostly in terms of increased vertical stability of the water column, that will hinder the deep ventilation of the hypolimnetic waters and will increase their actual water renewal time (Pilotti et al., 2014). Here we show that a further issue is provided by the growing inflow of nutrients following the intensification of storms. The results of the simulation conducted according to the modified rainfall series for the period 2007-2016 yield a 6.5% average yearly increase in CSO volumes. This increase is positively correlated with the natural variability of rainfall events during the year. For instance, during 2016, whose cumulated annual rainfall series is close to the long-term average but is characterized by single events more intense than usual, the total discharged volume increased up to 15% with respect to the average. This process would be further enhanced by a possible increase in the imperviousness of the urbanized areas. Moreover, an increased load of nutrients released in the summer period could also contribute to phytoplankton and cyanobacteria growth. Studies demonstrated that in Lake Maggiore rainfall stimulates the growth of phytoplankton and the development of summer blooms, likely due to a short term increase in nutrients when epilimnetic waters are usually nutrient depleted (Morabito et al., 2018).

From the operative point of view, the different patterns of the DCL curves computed at the two monitored CSWs show that first flush capture tanks, often expensive and difficult to build, are not necessarily the most suitable structural practice to tackle the problem posed by CSOs. Conversely, by reducing surface runoff, best practices in the drained watershed are generally an effective way to limit not only peak flows but also to curb pollution. The results also show that it is fundamental to limit the amount of infiltration waters, by implementing waterproofing practices on the existing network (by pipe monitoring, relining and introduction of flap valves on connections between the collector and the lake) and by searching for wrong connections and disconnecting runoff producing areas in relatively unpolluted urban environments along the tributary watersheds.

By repeating the 10 year simulation in the theoretical condition of negligible infiltration along the pipes network, the volumes discharged to the lake by the CSWs would decrease by 17%. It is worth underlining that, apart from the dominant environmental externalities, the groundwater infiltration increases management costs due to the energy used by the pumping stations to lift the water volumes. By running the model with and without infiltrations for the period 2007–2016, we calculated the operating time of each pump in both conditions. Knowing the operating times and the nominal power, obtained by using the characteristic curves of each pump, the yearly energy absorbed by the pumps in the real case, with and without infiltrations, was computed. By eliminating the infiltrations, a yearly average energy saving of 0.34 GWh could be obtained, that amounts to almost 20% of the overall energy consumption.

In addition, the implementation of a different management logic of the pumping stations would provide an appreciable improvement of the CSO scenario. Actually, a synergetic economic and environmental benefit would be obtained by changing the operative rule of the final pump station at S1. Since the activation of the PAR CSW is governed by the levels in the tank of the outlet pumping station S1 at Paratico, a possible strategy to improve the functioning of the sewer system would be to lower the startup and shutoff depth of the pumps in order to reduce the backwater effect in the downstream part of the main sewer. The model was eventually used to test the reduction in annual volumes discharged by PAR CSW that would be obtained by lowering the tank levels by 0.2 m and 0.8 m. The computed reduction is 36% in the first case and 66% in the second, with a slight increase in overall costs at pumping station S1 (2% and 5% respectively).

It is interesting to observe that an improved management of the sewer is beneficial, both in economic and environmental terms: from this perspective, the long-term simulation provides the quantification of the role of infiltrations on the reduction of the conveyance capacity of the system and, as a consequence, on the increase of the CSO volumes during wet weather.

Finally, the renewal of the urban environment in relatively unpolluted areas must be directed to the introduction of pervious materials, progressively introducing a sponge-city culture, that is a

fundamental step towards the protection of the fragile lake ecosystems.

5. Conclusion

In this paper the case of the Italian Lake Iseo was considered as an emblematic exemplification of a lake evolving towards eutrophic conditions. The study showed that, although the construction of a collector used to intercept and treat the urban sewage is a fundamental step to reduce the overall pollutant load discharged into a lake, the effectiveness of this solution in a combined sewer system is strongly compromised during wet weather periods. This is a critical problem of general interest, since the majority of existing sewer systems are combined and the separation of storm waters and waste waters is often economically and technically unsustainable. Until recently, even in fragile environments such as lakes, this nutrient source has often been overlooked, mostly due to the economic and practical difficulties involved in the systematic monitoring of spillways, and to the assumption that the combined sewer systems perform according to theoretical assumptions.

A year-long monitoring campaign on two combined sewer spillways and its generalization through an extensive simulation over a 10 year period show that in Lake Iseo the residual contribution amounts to about 20% (40%) of the total phosporous (nitrogen) load conveyed by the collector to the final waste water treatment plant. The generalization of the results to a "*business-as-usual*" climate change scenario, obtained by amplifying the most intense storms, keeping the cumulative yearly rainfall constant, demonstrated that it is reasonable to expect a further 10% increase in the computed volumes with respect to the overall values. In relative terms, in the particular case of this lake that drains a watershed that is 30 times larger than its area, these values could seem a minor contribution, although an extension of this study to the large watershed of Valle Camonica would certainly inflate the computed values. In other situations, this residual load can be dominant and contribute to explain the slow recovery of a lake from its eutrophic condition.

The results evidenced a further and relatively unknown way in which climate change will further challenge lakes. Although unexplored in this paper, similar consequences can be expected as a result of the growing urbanization on the watershed hydrology, a problem that is often considered only in terms of its effects on flood risk. This paper suggests that water quality is the other subtler (and possibly more difficult to solve) implication of this issue.

Moreover, the measurements showed the different behaviors of combined sewer spillways located along the tributary sewers and along the main collector. Whereas in the first case, the construction of water retention ponds would be justified due to the occurrence of first flush phenomenon, in the latter this intervention would be impaired by the stronger mixing that equalizes the pollutant concentration during rainfall events. The efficiency of flush storage tanks placed on the spillways of the main collector is actually diminished by the absence of the first flush phenomenon: accordingly, larger storage volumes would be needed to gain a satisfactory capture efficiency with respect to the possible location in the secondary tributary networks.

This result further underlines the site specific nature of the first flush phenomenon, even inside the same drainage network and the need to conduct extensive monitoring campaigns of overflows in terms of frequency, volume and mass of major pollutants, in order to have reliable estimates of the loads actually discharged through spillways. Moreover, these considerations emphasize the importance of limiting the residual nutrient loading entering a lake by using distributed non-structural practices aimed at diminishing the wet-period volumes.

Declaration of Competing Interest

The authors declare that they have no known competing financial interests or personal relationships that could have appeared to influence the work reported in this paper.

Acknowledgements

This research is part of the ISEO (Improving the lake Status from Eutrophy to Oligotrophy) project and was made possible by a CARIPLO foundation grant number 2015-0241. The project was financially supported also by Acque Bresciane – Servizio Idrico Integrato. In case of request for research purposes, Acque Bresciane will also provide the data made available for this paper. We are grateful to Manuel Murgioni for his valuable contribution to the activities that made this work possible. We acknowledge HydroPraxis for the University Grant PCSWMM licence that considerably simplified the modeling effort. Finally, we would like to thank the reviewers, whose valuable suggestions contributed to improve the quality of this paper.

Appendix 1. Quality assurance and quality control of chemical data

Phosphorus and nitrogen are key nutrients determined in most environmental monitoring and research programmes and only accurate analytical data permits valid conclusions to be drawn for load calculations. In order to assure a high quality standard and reproducibility of the total phosphorus (TP) and total nitrogen (TN) concentrations and respective loads along with chemical and biological oxygen demand, the sampling protocol, sample handling and analysis were performed according to standard methods (APHA, 2012; APAT-IRSA, 2003). Since the sampler was not refrigerated, the samples were retrieved within 2 to 3 hours after collection, immediately transferred into pre labelled, polyethylene bottles and transported within 2 hours in a cool box to the laboratory. In order to avoid cross contamination, all sampling containers were pre washed by soaking them overnight in a 10% HCl solution and then rinsed twice with distilled water. The quality control of the analyses was performed by constantly evaluating the performance of the full analytical procedures. All chemicals for reagents and standard preparations met the analytical reagent grade quality.

Once in laboratory, samples were analysed for TP and TN concentrations using standard spectrophotometric (Perkin Elmer, Lambda 35) methods after wet alkaline peroxydisulfate oxidation of the unfiltered sample (Valderrama, 1981). To do this, known volumes of unfiltered and homogenized samples were transferred into glass vials to which a solution of peroxydisulfate digestion reagent was added. The samples were then oxidized in an autoclave for 1 hour and after cooling at room temperature (20°C), they were analysed as soluble reactive phosphorus (APHA, 2012 Method 4500-P Ascorbic Acid Method) and nitrate (APHA, 2012 Method 4500-NO3 Cadmium Reduction Method). The spectrophotometer was regularly calibrated (bimonthly) for dissolved inorganic phosphorus (SRP) and nitrate (NO_3), by means of calibration curves made of six standard concentrations. Each standard concentration was prepared in triplicate. Five analytical blanks, that underwent the same digestion and analytical procedure as the samples, were always analysed to correct for sample contamination due to sample handling and reagent addition. Verification of the analytical method performance was carried out by analysing, at each sampling event, 3 analytical standards for SRP and nitrate NO_3. Standards were chosen approximately near the lower end (25 and 100 µg/L for SRP and NO_3 respectively), at the midpoint (100 and 1000 µg/L for SRP and NO_3 respectively) and at the highest

end (250 and 3000 µg/L for SRP and NO_3 respectively) of the analytical range. Response factor constancy over time was checked and recovery was between 95-105%. The accuracy of the oxidation procedure and of the calculated TN and TP concentrations were checked by analysing, on each event, three replicate standards of organic phosphorus and nitrogen of known concentration (adenosine triphosphate solution at 1.2 mg/L). In all samples TP and TN concentrations were significantly greater than the respective assay detection limits (20 and 50 µg/L for TP and TN respectively). Precision, at the relevant concentration ranges, was estimated as the relative standard deviation of 3 replicate analyses of the site water, and was 5% (TP) and 6% (TN).

Occasionally, samples were also analysed for COD (5 events), BOD5 (3 events) and total suspended solids TSS (2 events). In order to assure reproducibility of the results, sampling and handling procedures followed the same protocol as previously described. Samples for chemical oxygen demand (COD) were analysed by titration with ferrous ammonium sulfate after oxidation with chromic and sulfuric acids (APHA, 2012 Method 5220 C), while samples for biological oxygen demand (BOD5) were analysed as the change in dissolved oxygen concentration after a 5 day incubation in a stoppered bottle kept in the dark at 20°C (APHA, 2012 Method 5210 B). In order to prevent changes in the samples due to microbial activity, all the analysis initiated within 5 hours after the collection of the sample. The quality control of COD analyses was performed by always running three analytical blanks and three synthetic samples containing potassium hydrogen phthalate at a concentration of 0.4251 g/L. Response constancy over time was checked and recovery was above 95%. Precision, at the relevant concentration ranges, estimated as the relative standard deviation of 3 replicate analyses of the site water was 12%. The quality control of BOD5 analyses was performed by assuring an oxygen consumption $>$ 2.0 mg/L and an oxygen residual at the end of the incubation $>$ 1.0 mg/L. Precision, at the relevant concentration ranges, estimated as the relative standard deviation of 3 replicate analyses of the site water was 8.3%. Oxygen concentration was measured with an optical oxygen probe connected to a FireSting meter (Pyroscience) calibrated at 0 and 100% oxygen saturation according to manufacturer instructions. Total suspended solids (TSS) were determined by weight, as the dry mass of total solids retained after filtration and drying at 105°C of a well-mixed, measured volume of a water sample through a pre weighed 0.4 um membrane filter (Whatman TM) (APAT-IRSA, 2003). The weight was measured with an analytical balance capable of weighing 0.1 mg and regularly calibrated using reference standard weights.

References

APAT-IRSA, CNR, 2003. Metodi analitici per le acque. Manuali e Linee. APAT-IRSA CNR, Roma.

edited by APHA, 2012. Standard methods for the examination of water and wastewater. In: Rice, E.W., Baird, R.B., Eaton, A.D., Clesceri, L.S. (Eds.), American Water Works Association (AWWA) and Water Environment Federation (WEF), 22nd edition American Public Health Association (APHA), Washington, D.CUSA.

Bach, P.M., McCarthy, D.T., Deletic, A., 2010. Redefining the stormwater first flush phenomenon. Water Res. 44 (8), 2487–2498.

Baek, S.-., Choi, D.-., Jung, J.-., Lee, H.-., Lee, H., Yoon, K.-., Cho, K.H., 2015. Optimizing low impact development (LID) for stormwater runoff treatment in urban area, korea: Experimental and modeling approach. Water Res. 86 122–131. doi:10.1016/j.watres.2015.08.038.

Barone, L., Pilotti, M., Valerio, G., Balistrocchi, M., Milanesi, L., Chapra, S.C., Nizzoli, D., 2019. Analysis of the residual nutrient load from a combined sewer system in a watershed of a deep Italian lake. J. Hydrol. 571, 202–213. doi:10.1016/j.jhydrol.2019.01.031.

Balistrocchi, M., Grossi, G., Bacchi, B., 2009. An analytical probabilistic model of the quality efficiency of a sewer tank. Water Resour. Res. 45 (12), W12420. doi:10.1029/2009WR007822.

Balistrocchi, M., Grossi, G., 2020. Predicting the impact of climate change on urban drainage systems in northwestern Italy by a copula-based approach. J. Hydrol. Regional Study 28, 100670. doi:10.1016/j.ejrh.2020.100670.

Bertrand-Krajewski, J.L., Chebbo, G., Saget, A., 1998. Distribution of pollutant mass vs volume in stormwater discharges and the first flush phenomenon. Water Res. 32 (8), 2341–2356.

Bonomi, G., Gerletti, M., 1967. Il Lago d'Iseo: primo quadro limnologico generale (termica, chimica, plancton e benton profondo). Mem. Ist. Ital. Idrobiol. 22, 149–175.

Bravo, H.R., McLellan, S.L., Klump, J.V., Hamidi, S.A., Talarczyk, D., 2017. Modeling the fecal coliform footprint in a Lake Michigan urban coastal area. Environ. Model. Softw. 95, 401–419.

Bryan Ellis, J., Yu, W., 1995. Bacteriology of urban runoff: The combined sewer as a bacterial reactor and generator. Water Sci. Technol. 31 (7), 303–310.

Camargo, J.A., Alonso, A., 2006. Ecological and toxicological effects of inorganic nitrogen pollution in aquatic ecosystems: a global assessment. Environ. Int. 32, 831–849.

Chebbo, G., Gromaire, M.C., Ahyerre, M., Garnaud, S., 2001. Production and transport of urban wet weather pollution in combined sewer systems: the "Marais" experimental urban catchment in Paris. Urban Water 3 (1–2), 3–15.

Chen, L., Dai, Y., Zhi, X., Xie, H., Shen, Z., 2018. Quantifying nonpoint source emissions and their water quality responses in a complex catchment: A case study of a typical urban-rural mixed catchment. J. Hydrol. 559, 110–121.

Dai, C., Tan, Q., Lu, W.T., Liu, Y., Guo, H.C., 2016. Identification of optimal water transfer schemes for restoration of a eutrophic lake: An integrated simulation-optimization method. Ecol. Eng. 95, 409–421.

Deletic, A., 1998. The first flush load of urban surface runoff. Water Res.32 (8) 2462–2470.

Ekanayake, D., Aryal, R., Hasan Johir, M.A., Loganathan, P., Bush, C., Kandasamy, J., Vigneswaran, S., 2019. Interrelationship among the pollutants in stormwater in an urban catchment and first flush identification using UV spectroscopy. Chemosphere 233, 245–251. doi:10.1016/j.chemosphere.2019.05.285.

Farnan, J.C., Sobanski, J.P., Venuso, N., Gronski, A., 2004. Chicago's deep tunnel - history and evolution. Proceedings of the Water Environment Federation, 577-584. 10.2175/193864704784107380.

Fortier, C., Mailhot, A., 2015. Climate change impact on combined sewer overflows. J. Water Resour. Plan. Manage. 141 (5) (May 2015).

Francey, M., Fletcher, T.D., Deletic, A., Duncan, H., 2010. New insights into the quality of urban storm water in south eastern australia. J. Environ. Eng. 136 (4), 381–390. doi:10.1061/(ASCE)EE.1943-7870.0000038.

Frazar, S., Gold, A.J., Addy, K., Moatar, F., Birgand, F., Schroth, A.W., . . . Pradhanang, S.M, 2019. Contrasting behavior of nitrate and phosphate flux from high flow events on small agricultural and urban watersheds. Biogeochemistry 145 (1-2), 141–160. doi:10.1007/s10533-019-00596-z.

Garibaldi, L., Brizzio, M.C., E Mosello R., Mezzanotte V., 1997. Apporti di fosforo al Sebino: confronto framisuresperimentali e teoriche. Acqua Aria 30 (11-12), 105–110.

Garibaldi, L., V. Mezzanotte, M.C., Brizzio, M.Rogora, R, Mosello, 1999. The trophic evolution of Lake Iseo as related to its holomixis. J. Limnol. 62, 10–19.

Ghirardi, N., Bolpagni, R., Bresciani, M., Valerio, G., Pilotti, M., Giardino, C., 2019. Spatiotemporal dynamics of submerged aquatic vegetation in a deep lake from Sentinel-2 data. Water 11, 563. doi:10.3390/w11030563.

Gikas, G.D., Tsihrintzis, V.A., 2012. Assessment of water quality of first-flush roof runoff and harvested rainwater. J. Hydrol. 466-467 115–126. doi:10.1016/j.jhydrol.2012.08.020.

Gironás, J., Roesner, L.A., Rossman, L.A., Davis, J., 2010. A new applications manual for the Stormwater Management Model (SWMM). Environ. Model. Softw. 25 (6), 813–816.

Gnecco, I., Berretta, C., Lanza, L.G., La Barbera, P., 2005. Storm water pollution in the urban environment of genoa. Atmos. Res. 77 (1–4 SPEC. ISS.), 60–73. doi:10.1016/j.atmosres.2004.10.017.

IPCC, 2014. In: Pachauri, R.K., Meyer, L.A. (Eds.), Contribution of Working Groups I, II and III to the Fifth Assessment Report of the Intergovernmental Panel on Climate Change. IPCC, Geneva, SW.

Jenny, Jean-Philippe, Anneville, Orlane, Arnaud, Fabien, Baulaz, Yoann, Bouffard, Damien, Domaizon, Isabelle, Serghei, A, 2020. Bocaniov, Nathalie Chèvre, Maria Dittrich, Jean-Marcel Dorioz, Erin S. Dunlop, Gaël Dur, Jean Guillard, Thibault Guinaldo, Stéphan Jacquet, Aurélien Jamoneau, Zobia Jawed, Erik Jeppesen, Gail Krantzberg, John Lenters, Barbara Leoni, Michel Meybeck, Veronica Nava, Tiina Nõges, Peeter Nõges, Martina Patelli, Victoria Pebbles, Marie-Elodie Perga, Serena Rasconi, Carl R. Ruetz, Lars Rudstam, Nico Salmaso, Sharma Sapna, Dietmar Straile, Olga Tammeorg, Michael R. Twiss, Donald G. Uzarski, Anne-Mari Ventelä, Warwick F. Vincent, Steven W. Wilhelm, Sten-Åke Wängberg, Gesa A. Weyhenmeyer, Scientists' Warning to Humanity: Rapid degradation of the world's large lakes. J. Great Lakes Res. 46 (4), 686–702. doi:10.1016/j.jglr.2020.05.006, ISSN 0380-1330.

Kidmose, J., Troldborg, L., Refsgaard, J.C., Bischoff, N., 2015. Coupling of a distributed hydrological model with an urban storm water model for impact analysis of forced infiltration. J. Hydrol. 525, 506–520.

Huang, D.-B., Bader, H.-P., Scheidegger, R., Schertenleib, R., Gujer, W, 2007. Confronting limitations: New solutions required for urban water management in Kunming City. J. Environ. Manage. 84 (1), 49–61.

Houhou, J., Lartiges, B.S., France-Lanord, C., Guilmette, C., Poix, S., Mustin, C., 2010. Isotopic tracing of clear water sources in an urban sewer: a combined water and dissolved sulfate stable isotope approach. Water Res. 44, 256e266.

Karpf, C., Krebs, P., 2011. Quantification of groundwater infiltration and surface water inflows in urban sewer networks based on a multiple model approach. Water Res. 45 (10), 3129–3136.

Kaushal, S.S., Groffman, P.M., Band, L.E., Elliott, E.M., Shields, C.A., Kendall, C., 2011. Tracking nonpoint source nitrogen pollution in human-impacted watersheds. Environ. Sci. Tech. 45 (19), 8225–8232. doi:10.1021/es200779e.

Kim, G., Yur, J., Kim, J., 2007. Diffuse pollution loading from urban stormwater runoff in Daejeon city, Korea. J. Environ. Manage. 85 (1), 9–16. doi:10.1016/j.jenvman.2006.07.009.

Liu, Y., Wang, Y., Sheng, H., Dong, F., Zou, R., Zhao, L., Guo, H., Zhu, X., He, B., 2014. Quantitative evaluation of lake eutrophication responses under alternative water diversion scenarios: A water quality modeling based statistical analysis approach. Sci. Total Environ. 468-469, 219–227.

Lund, A., McMillan, Joseph, Kelly, Rosmarie, Jabbarzadeh, Shirin, Mead, Daniel G, Burkot, Thomas R, Kitron, Uriel, Vazquez-Prokopec, Gonzalo M, 2014. Long term impacts of combined sewer overflow remediation on water quality and population dynamics of Culex quinquefasciatus, the main urban West Nile virus vector in Atlanta. Environ. Res. 129, 20–26.

Ma, Z.-B, Ni, H.-G., Zeng, H., Wei, J.-B., 2011. Function formula for first flush analysis in mixed watersheds: A comparison of power and polynomial methods. J. Hydrol. 402 (3-4), 333–339.

Madoux-Humery, AS, Dorner, S, Sauvé, S, et al., 2013. Temporal variability of combined sewer overflow contaminants: evaluation of wastewater micropollutants as tracers of fecal contamination. Water Res. 47 (13), 4370–4382. doi:10.1016/j.watres.2013.04.030.

Mamoon, A.A., Jahan, S., He, X., Joergensen, N.E., Rahman, A., 2019. First flush analysis using a rainfall simulator on a micro catchment in an arid climate. Sci. Total Environ. 693 doi:10.1016/j.scitotenv.2019.07.358.

Marsalek, J., Chocat, B., 2002. International report: Stormwater management. Water Sci. Tech. 46 (6–7), 1–17.

Marsalek, J., 2003. Overview of urban stormwater impacts on receiving waters. In: Arsov, R., Marsalek, J., Watt, E., Zeman, E. (Eds.), Urban Water Management: Science Technology and Service Delivery. NATO Science Series (Series IV: Earth and Environmental Sciences), eds. Springer, Dordrecht vol. 25.

Matsui, S., Ide, S., Ando, Lakes, M., 1995. Lakes and reservoirs: Reflecting waters of sustainable use. Water Sci. Tech. 32 (7), 221–224. doi:10.1016/0273-1223(96)00068-6, ISSN 0273-1223.

McLellan, S.L., Hollis, E.J., Depas, M.M., Van Dyke, M., Harris, J., Scopel, C.O., 2007. Distribution and fate of Escherichia coli in Lake Michigan following contamination with urban storm- water and combined sewer overflows. J. Great Lakes Res. 33 (3), 566–580.

McCrackin, M.L., Jones, H.P., Jones, P.C., Moreno-Mateos, D., March 2017. Recovery of lakes and coastal marine ecosystems from eutrophication: A global meta-analysis. Limnol. Ocean. 62 (2), 507–518 1.

Meals, D.W., Budd, L.F., 1998. Lake Champlain Basin nonpoint source phosphorus assessment. J. Am. Water Res. Assoc. 34 (2), 251–265.

Moore, J.W., Schindler, D.E., Scheuerell, M.D., Smith, D., Frodge, J., February 2003. Lake eutrophication at the urban fringe, Seattle region. Ambio 32 (1), 13–18.

Morabito, G., Manca, M., 2014. Eutrophication and recovery of the large and deep subalpine lake maggiore: patterns, trends and interactions of planktonic organisms between trophic and climatic forcings. In: Lambert, A., Roux, C. (Eds.), Eutrophication: Causes, Economic Implications and Future Challenges. NOVA Publishers, New York.

Morabito, G., Rogora, M., Austoni, M., et al., 2018. Could the extreme meteorological events in Lake Maggiore watershed determine a climate-driven eutrophication process? Hydrobiologia 824, 163–175. doi:10.1007/s10750-018-3549-4.

Müller, G., Clear Constance, Water QualityInternational, Volume 1997, Issue 9-10, 1997, 30-33.

Nie, L., Lindholm, O., Lindholm, G., Syversen, E., 2009. Impacts of climate change on urban drainage systems – a case study in Fredrikstad. Urban Water J. 6 (4), 323–332. doi:10.1080/15730620802600924.

Novotny, V., Goodrich-Mahoney, J., 1978. Comparative assessment of pollution loadings from non-point sources in urban land use. Progress Water Technol. 10, 775–785.

Obropta, C.C., Kardos, J.S., 2007. Review of urban stormwater quality models: Deterministic, stochastic, and hybrid approaches. J. Am. Water Resour. Assoc. 43 (6), 1508–1523. doi:10.1111/j.1752-1688.2007.00124.x.

OECD (Organisation for Economic Co-Operation and Development), 1982. Eutrophication of Waters. Monitoring, Assessment and Control, 42077. 154 pp. publication N°, Paris.

Paul, M.J., Meyer, J.L., 2001. Streams in the urban landscape. Annu. Rev. Ecol. Syst. 32, 333–365.

Pena-Regueiro, J., Sebastiá-Frasquet, M.-T., Estornell, J., Aguilar-Maldonado, J.A., 2020. Sentinel-2 application to the surface characterization of small water bodies in wetlands. Water 12, 1487.

Perera, T., McGree, J., Egodawatta, P., Jinadasa, K.B.S.N., Goonetilleke, A., 2019. Taxonomy of influential factors for predicting pollutant first flush in urban stormwater runoff. Water Res. 166 doi:10.1016/j.watres.2019.115075.

Pilotti, M., Simoncelli, S., Valerio, G., 2014. A simple approach to the evaluation of the actual water renewal time of natural stratified lakes. Water Resour. Res. 50 (4), 2830–2849. doi:10.1002/2013WR014471.

Pretty, J.N., Mason, C.F., Nedwell, D.B., Hine, R.E., Leaf, S., Dils, R., 2003. Environmental costs of freshwater eutrophication in England and Wales. Environ. Sci. Technol. 37, 201–208. doi:10.1021/es020793k.

Rapin, F., Gerdeaux, D., December 2013. Control of eutrophication in Lake Geneva [La protection du Léman priorité à la lutte contre l'eutrophisation]. Arch. des Sci. 66 (2), 103–116.

Razak Irwan, A., Christensen Erik, R., 2001. Water quality before and after deep tunnel operation in Milwaukee. Wat. Res. 35 (11), 2683–2692.

Rossman, L.A., 2015. Storm water management model user's manual, version 5.1. National Risk Management Research Laboratory. Office of Research and Development. US Environmental Protection Agency, Cincinnati.

Salerno, F., Viviano, G., Tartari, G., 2018. Urbanization and climate change impacts on surface water quality: Enhancing the resilience by reducing impervious surfaces. Water Res. 144, 491–502.

Sansalone, J.J., Cristina, C.M., 2004. First flush concepts for suspended and dissolved solids in small impervious watersheds. J. Environ. Eng. 130 (11), 1301–1314.

Schindler, D.W., 1977. Evolution of phosphorus limitation in lakes. Science 195, 260–262. doi:10.1126/science.195.4275.260.

Schindler, D.W., 2006. Recent advances in the understanding and management of eutrophication. Limnol. Oceanogr. 51 (1, part 2), 356–363.

Schindler, D.W., 2012. The dilemma of controlling cultural eutrophication of lakes. Proc. Biol. Sci. 279, 4322–4333. doi:10.1098/rspb.2012.1032.

Sebastiá-Frasquet, M.-T., Rodilla, M., Falco, S., Sanchis, J.-A., 2013. Analysis of the effects of wet and dry seasons on a Mediterranean river basin: Consequences for coastal waters and its quality management. Ocean Coast. Manage. 78, 45–55. doi:10.1016/j.ocecoaman.2013.03.012. ISSN 0964-5691 http://www.sciencedirect.com/science/article/pii/S0964569113000793 .

Semadeni-Davies, A., Hernebring, C., Svensson, G., Gustafsson, L.G., 2008. The impacts of climate change and urbanisation on drainage in Helsingborg, Sweden: Combined sewer system. J. Hydrol. 350 (1–2), 100–113. doi:10.1016/j.jhydrol.2007.05.028, IssuesISSN 0022-1694.

Sinha, E., Michalak, A.M., Balaji, V., 2017. Eutrophication will increase during the 21st century as a result of precipitation changes. Science 357, 405–408.

Smil, V., 2000. Phosphorus in the environment: natural flows and human interferences. Annu. Rev. Energy Environ. 25, 53–88.

Staufer, P., Scheidegger, A., Rieckermann, J., 2012. Assessing the performance of sewer rehabilitation on the reduction of infiltration and inflow. Water Res. 46 (16), 5185–5196. doi:10.1016/j.watres.2012.07.001.

Tang, Z., Engel, B.A., Pijanowski, B.C., Lim, K.J., 2005. Forecasting land use change and its environmental impact at a watershed scale. J. Environ. Manage. 76 (1), 35–45. doi:10.1016/j.jenvman.2005.01.006.

Tibbetts, J., 2005. Combined sewer systems: down, dirty and out of date. Environ. Health Perspect. 113, A464–A467.

U.S. Environmental Protection Agency (USEPA), 2009. National Lakes Assessment: A Collaborative Survey of the Nation's Lakes. EPA 841-R-09-001. U.S. Office of Water and Office of Research and Development. Environmental Protection Agency, Washington, D.C.

US Environmental Protection Agency (USEPA), 2009. National Water Quality Inventory: Report to Congress. US Environmental Protection Agency, Washington, DC Available from: http://water.epa.gov/lawsregs/guidance/cwa/305b/upload/2009_01_22_305b_2004report_2004_305Breport.pdf .

Valderrama, J.C., 1981. The simultaneous analysis of total nitrogen and total phosphorus in natural waters. Mar. Chem. 10 (2), 109–122.

Valerio, G., Pilotti, M., Barontini, S., Leoni, B., 2015. Sensitivity of the multiannual thermal dynamics of a deep pre-alpine lake to climatic change. Hydrol. Process. 29 (5), 767–779. doi:10.1002/hyp.10183.

Vollenweider, R.A., 1975. "Input-output models with special reference to phosphorus loading concept in limnology," Schweizerische Zeitschrift fur Hydrologie-Swiss. J. Hydrol. 37, 53–84.

Walsh, C.J., Roy, A.H., Feminella, J.W., Cottingham, P.D., Groffman, P.M., Morgan, R.P., 2005. The urban stream syndrome: current knowledge and the search for a cure. J. North Am. Benthol. Soc. 24, 706–723.

Watson, S.B., Miller, C., Arhonditsis, G., Boyer, G.L., Carmichael, W., Charlton, M.N., Confesor, R., Depew, D.C., Höök, T.O., Ludsin, S.A., Matisoff, G., McElmurry, S.P., Murray, M.W., Peter Richards, R., Rao, Y.R., Steffen, M.M., Wilhelm, S.W, 2016. The re-eutrophication of Lake Erie: Harmful algal blooms and hypoxia. Harmful Algae 56, 44–66.

Welch, EB., 1981. The diversion/dilution technique in lake restoration. Water Resour. Bull. 17, 558–564.

Wilander, A., Persson, G., Recovery from eutrophication: Experiences of reduced phosphorus input to the four largest lakes of Sweden Ambio, Volume 30, Issue 8, 2001, Pages 475-485

Xu, Z., Yin, H., Li, H., 2014. Quantification of non-stormwater flow entries into storm drains using a water balance approach. Sci. Total Environ. 487 (1), 381–388.